

A TURBO DETECTION SCHEME FOR EGPRS

A THESIS SUBMITTED TO
THE GRADUATE SCHOOL OF NATURAL AND APPLIED SCIENCES
OF
THE MIDDLE EAST TECHNICAL UNIVERSITY
BY

ÜLKÜ GÜLMEZ BAŞKÖY

IN PARTIAL FULFILLMENT OF THE REQUIREMENTS FOR THE
DEGREE OF
MASTER OF SCIENCE
IN
THE DEPARTMENT OF ELECTRICAL AND ELECTRONICS
ENGINEERING

SEPTEMBER 2003

Approval of the Graduate School of Natural and Applied Sciences

Prof. Dr. Canan ÖZGEN

Director

I certify that this thesis satisfies all the requirements as a thesis for the degree of Master of Science.

Prof. Dr. Mübeccel DEMİREKLER

Head of Department

This is to certify that we have read this thesis and that in our opinion it is fully adequate, in scope and quality, as a thesis for the degree of Master of Science.

Assoc. Prof. Dr. Buyurman BAYKAL

Supervisor

Examining Committee Members

Assoc. Prof. Dr. Melek D. YÜCEL

Assoc. Prof. Dr. Tolga ÇİLOĞLU

Assoc. Prof. Dr. Buyurman BAYKAL

Assoc. Prof. Dr. Engin TUNCER

M.Sc. Hacer SUNAY (TÜBİTAK-BİLTEN)

ABSTRACT

A TURBO DETECTION SCHEME FOR EGPRS

Başköy Gülmez, Ülkü

M.Sc., Department of Electrical and Electronics Engineering

Supervisor : Assoc. Prof. Dr. Buyurman Baykal

September 2003, 71 pages

Enhanced Data Rates for Global Evolution (EDGE) is one of the 3G wireless communication standards, which provides higher data rates by adopting 8-PSK modulation in TDMA system infrastructure of GSM. In this thesis, a turbo detection receiver for Enhanced General Packet Radio Services (EGPRS) system, which is the packet switching mode of EDGE, is studied. In turbo detection, equalization and channel decoding are performed iteratively. Due to 8-ary alphabet of EGPRS modulation, full state trellis based equalization, as usually performed in GSM, is too complex not only for turbo detection but even for conventional equalization; so suboptimum schemes have to be considered. The Delayed Decision Feedback Sequence Estimation (DDFSE) is chosen as suboptimal and less complex trellis based

scheme and it is examined as a conventional equalization technique firstly. It is shown that the DDFSE has a fine tradeoff between performance and complexity and can be a promising candidate for EGPRS. Then it is employed to reduce the number of the trellis state in turbo detection. Max-log-MAP algorithm is used for soft output calculations of both SISO equalizer and SISO decoder. Simulation results illustrate that proposed turbo detection structure improves bit error rate and block error rate performance of the receiver with respect to the conventional equalization and decoding scheme. The iteration gain varies depending on modulation type and coding rate of Modulation Coding Scheme (MCS) employed in EGPRS.

Keywords: Equalization, Decoding, Turbo Detection, Delayed Decision Feedback Sequence Estimation (DDFSE), Enhanced Data Rates for Global Evolution (EDGE), Enhanced General Packet Radio Services (EGPRS).

ÖZ

GGPRS İÇİN BİR TURBO SEZİMİ YAPISI

Başköy Gülmez, Ülkü

Yüksek Lisans, Elektrik ve Elektronik Mühendisliği Bölümü

Tez Yöneticisi : Doç. Dr. Buyurman Baykal

Eylül 2003, 71 sayfa

Küresel evrim için geliştirilmiş veri hızı, yüksek bilgi akışı sağlayan üçüncü jenerasyon kablosuz iletişim standartlarından biridir. 8 PSK kipleme tekniğini GSM'in zaman bölümlü çoğul erişim altyapısında kullanır. Bu tezde Küresel Evrim için Geliştirilmiş Veri Hızı'nın paket anahtarlama modu olan Geliştirilmiş Genel Paket Radyo Servisleri (GGPRS) için turbo sezimi ile çalışan bir alıcı üzerinde çalışılmıştır. Turbo sezim yöntemi kanal şifrelemesini çözme ve denkleştirme işlemini döngülü olarak yapar ve alıcı performansını yükseltir. Genellikle GSM için kullanılan tam durumlu kafes tabanlı denkleştirme yöntemini turbo sezimi için kullanmak GGPRS'in uyguladığı 8 PSK kiplemesi düşünüldüğünde oldukça yüksek bir hesaplama karmaşıklığı yaratır. Ki bu yapının alışlagelmiş denkleştirme ve şifre

özümleme yöntemi için bile uygulanması oldukça zordur. Bu nedenle yarı uygun yapılar GGPRS için düşünölmelidir. Geciktirilmiş Karar Geribeslemeli Dizi Kestirme (GKGDK) yarı uygun ve daha az hesaplama karmaşıklığı sunan kafes tabanlı yapı olarak seçilmiştir. GKGDK için performans ve hesaplama karmaşıklığı arasında uygulanabilir bir ilişki olduğu gösterilmiş ve GKGDK'nin GGPRS denkleştirme için uygun bir aday olabileceğı görölmüştür. Turbo seziminde kafes durumlarının azaltılması için GKGDK algoritması, yumuşak girdi/çıkııı sezim ve şifre çözme işlemleri için de Max-Log-MAP algoritması uygulanmıştır. Benzetim sonuçları göstermiştir ki uygulanan turbo sezimi yapısı GGPRS alıcısının bit hata oranını azaltmıştır. Döngölü kazanç, GGPRS'de kullanılan kipleme çeşidine ve şifreleme oranına göre değişmektedir.

Anahtar Kelimeler: Denkleştirme, Şifre Çözümleme, Turbo Sezimi, Geciktirilmiş Karar Geribeslemeli Dizi Kestirme (GKGDK), Küresel Evrim için Geliştirilmiş Veri Hızı, Geliştirilmiş Genel Paket Radyo Servisleri (GGPRS).

ACKNOWLEDGMENTS

I would like to express my gratitude to Assoc. Prof. Dr. Buyurman Baykal for his supervision.

I would like to thank to my husband for his assistance, unwavering support and patience. Also, special thanks to my family; my father İrfan Zeki Gülmez, my mother Sariye Gülmez, my sister Hande Gülmez and my brother Oğuzhan Gülmez for their great love and support through my whole education.

TABLE OF CONTENTS

ABSTRACT	iii
ÖZ	v
ACKNOWLEDGEMENTS	vii
TABLE OF CONTENTS	viii
CHAPTER	
1. INTRODUCTION	1
2. EQUALIZATION TECHNIQUES	6
2.1 Overview of equalization techniques	6
2.2 Maximum Likelihood Sequence Estimation	10
2.3 Delayed Decision-Feedback Sequence Estimation (DDFSE)	12
2.4 Computational Complexity Comparison of MLSE and DDFSE Algorithms	16
3. TURBO EQUALIZATION	19
3.1 Turbo Principle	20
3.2 SISO Decoding/Equalization	24
3.2.1 MAP Decoding Algorithms	25
3.2.2 SISO Decoder	30
3.2.3 SISO Equalizer	33

4. EQUALIZATION AND TURBO DETECTION FOR EGPRS	36
4.1 Modulation Coding Schemes of EGRRS	40
4.1.1 Modulation Format of EGPRS	42
4.1.1.1 Gaussian minimum-shift keying.....	42
4.1.1.2 8-ary Phase Shift Keying.....	44
4.2 Mobile Radio Channel.....	46
4.3 Receiver Structure	50
4.3.1 Channel Estimation	51
4.3.2 Delayed Decision Feedback Sequence Estimation for EGPRS..	53
4.3.3 Turbo Detection for EGPRS.....	59
5. CONCLUSION	65
REFERENCES	67

CHAPTER 1

INTRODUCTION

In the last decade, mobile communications has become one of the fastest growing markets especially with the introduction of the sophisticated digital cellular systems, “second generation” mobile radio systems. The global system for mobile communications (GSM) is one of the second-generation standards, which has been a major success story for the global telecommunications industry, delivering telephony and low bit-rate data services to mobile end-users. As of April 2002, for example, more than 180 countries accessed GSM to provide service to more than 680 million customers [1].

Today, several GSM-networks have almost reached their limits, i.e. the allocated spectrum is not sufficient to support the growing demand for mobile communications. Additionally, the demand for more transmission capacity is accelerated because of the growth in required high data high rates for new services in wireless communication, e.g. multimedia applications and the Internet.

The need for higher data rates is fulfilled by specifying standards within GSM phase 2+, called as General Packet Switched Services (GPRS) and High-Speed Circuit Switched Data (HSCSD) as a first evolution step in GSM [2][3]. These standards increase the spectral efficiency of GSM by employing multi-slot operations, hence their capacity of providing the higher transmission data rate is limited and more sophisticated approaches are soon required to meet the demand for faster access for information.

Since the early 1990s, industry has been actively researching third-generation mobile radio access systems and the standardization of the first release of third generation cellular systems was finalized in 1999 by ETSI/3GPP. Global system for mobile communication/enhanced data rates for global evolution (GSM/EDGE) is one of the third generation cellular systems specified by this standardization framework. EDGE is actually an evolution of the GSM and other TDMA based 2G mobile radio standards, i.e., IS-136, toward significantly higher spectral efficiency with a novel common physical layer and some upper layer features. Rapid availability, the reuse of existing GSM and TDMA infrastructure and high spectral efficiency make GSM/EDGE potentially attractive as a 3G migration path.

EDGE¹ improves the spectral efficiency by applying the modulation format 8-ary phase-shift keying (8 PSK), in conjunction with gaussian minimum-shift keying (GMSK) already used in GSM. The modification of the modulation scheme is of significant for equalization that fights against strong

¹ Although EDGE is a generic air interface, it is predominantly used in conjunction with GSM as Enhanced Data Rates for GSM evolution (EDGE)

channel inter-symbol interference (ISI) caused by limited bandwidth and multi-path propagation. Optimum equalization for minimizing bit error rate, i.e., maximum likelihood sequence estimation (MLSE) based on Viterbi algorithm, which is usually utilized for GSM, requires an extensive computational complexity due to increase in modulation size. Simpler schemes like Decision Feedback Estimation (DFE) tend to perform poorly for 8 PSK since the symbol constellation is fairly dense causing the algorithm to become overly sensitive to noise [11]. In this scenario, the Delayed Decision Feedback Sequence Estimation (DDFSE) seems to be an attractive candidate since it generates a tradeoff between complexity and performance. Additionally, it is well suited for implementation because of its high regularity.

Significant improvements in BER performance are possible with coded data transmission using channel coding. The basic idea of channel coding is to introduce controlled redundancy into the transmitted signals that is exploited at the receiver to correct channel induced errors by means of forward error correction. Conventional receivers generally involve equalization and channel decoding separately. In 1995, a new approach called as turbo detection has been proposed to efficiently combat strong ISI [12]. The basic idea consists in considering the channel as a non-recursive, non-systematic convolutional code of rate one and realizing a joint iterative channel equalization and decoding technique, whereby the channel decoder is utilized in order to improve the performance of the equalization process and vice versa in an iterative regime.

The scope of this thesis is to implement a turbo detection scheme to examine the performance of the turbo detection for modulation coding schemes of

EGPRS; the packet switched mode of EDGE, with a reduced complexity equalizer. For this purpose, the DDFSE is employed as the equalization technique for 8-PSK modulation and the tradeoff between the performance and complexity in mobile radio channel conditions are examined. Then, the performance of turbo detection for EGPRS, is studied with the DDFSE approach used in equalization part of turbo detection. The implementation is performed with C programming languages in the development environment of Microsoft Visual Studio 6.0.

In Chapter 2, an overview of equalisation techniques for TDMA systems is given and the Maximum Likelihood Sequence Estimation (MLSE) with the Delayed Decision Feedback Sequence Estimation (DDFSE) equalization algorithm is described in details. In order to obtain a meaningful comparison for the computational complexity of the MLSE and the DDFSE algorithms, an analysis for the computational complexity is also produced in this section.

In Chapter 3, the principle of turbo detection is first examined. Then, the MAP algorithm and its variants, log-MAP and Max-log-MAP are described. The soft in/ soft out (SISO) equalizer and channel decoder components, which utilize the MAP algorithms, are studied finally.

The application of the DDFSE and turbo detection to EGPRS is studied in Chapter 4. After a short introduction to EGPRS, modulation and coding schemes as well as mobile radio channels are treated. Then channel impulse response estimation and prefiltering for DDFSE are discussed. DDFSE equalization performance is investigated for GSM channel profiles. Finally, turbo detection performance is studied by applying turbo principle to EGPRS Modulation Coding Schemes (MCS).

In Chapter 5, some conclusions are drawn for DDFSE and turbo detection performance of the proposed receiver structure and some possible future work areas are pointed out.

CHAPTER 2

EQUALIZATION TECHNIQUES

Transmission through a band limited channel is an example of significant interest practically where the transmitted signal is distorted in time by the channel. The dispersion introduced by such a channel can cause interference between the transmitted adjacent symbols, which is called as Inter Symbol interference (ISI). In this case, the instantaneous signal in the receiver is visualized as superposition of several symbols in the past and in the future. In order to facilitate the reliable detection of signals corrupted by ISI, some form of ISI compensation, i.e. equalization, is required in the receiver. Equalisation techniques for digital modulation have received extensive attention in the literature for many years. It is beyond the scope of this thesis to address all these developments in detail, rather an overview will be provided of the most important equalization techniques. And the descriptions of the MLSE and DDFSE algorithms are expressed in subsections.

2.1 Overview of equalization techniques

Two broad categories of equalizers have been documented extensively in the literature; symbol-by-symbol equalizers and sequence estimators. *Symbol-by-*

symbol equalizers try to compensate ISI directly and to make symbol by symbol decisions on the received sequence, while *sequence estimators* attempt to find the most probably transmitted sequence regarding received sequence as a whole [8]. Sequence estimators are generally more complex than symbol-by-symbol equalizers, but can potentially offer better performances.

Linear equalizers and decision feedback equalizers are two broad categories of symbol by symbol equalizers. The first one, *linear equalizer* (LE), is the classic starting point for equalization. It is an essentially simple and intuitive solution to the problem of ISI elimination. Conceptually one applies a filter with the frequency response, which is the inverse of the channel, thereby creating a system with an ideal effective frequency response. The filter coefficients of the LE can be determined by zero forcing criteria, leading to Zero Forcing Linear Equalization (ZF-LE) or by Mean Square Error criteria, leading to Mean Square Error Linear Equalization (MSE-LE). In ZF-LE, the equalizer coefficients are chosen so as to force the combined channel and equalizer impulse response to zero at all but one of sampling instants in the span of the equalizer. In the MSE-LE, however, the coefficients are chosen to minimize the mean-square error at the output of the equalizer, so it takes into account ISI and noise together. Since the basic operation of the ZF equalizer is to provide gain at frequencies where the channel transfer function experiences attenuation and vice versa, both signal and noise are enhanced simultaneously. This results in noise enhancement, which degrades the performance of equalizer significantly. Even more, if channel has zeros on the unit circle (corresponding to infinite attenuation in the channel frequency response), the mean square error at the output of the equalizer becomes infinite. MSE-LE jointly minimizes the noise and the ISI, hence yields a

lower total min square error [9]. Additionally, the MSE-LE exists for the channels that exhibit spectral nulls since transfer function of the equalizer does not have corresponding poles. However, at higher SNR levels, when the noise contribution is low, the MSE equation of the MSE linear equalizer approaches that of the ZF linear equalizer, causing both the MSE and ZF equalizers to exhibit similar characteristics.

The problem of the noise enhancement in LEs' is greatly reduced by the *Decision Feedback Equalization* (DFE), the second category of the symbol by symbol equalizers. The DFE employs two filter, a feedforward filter and feedback filter, in order to eliminate the ISI. The non-linear function due to the decision device is introduced at the input of the feedback filter. The feedforward filter is fed only with present and future received signal samples and eliminates only the pre-cursor ISI. The feedback works with the estimates of the received samples from the decision device and mitigates the ISI caused by the past data symbols, i.e. the post-cursor ISI. Since the feedforward filter eliminates ISI partially and the feedback filter works only with estimated symbols, noise enhancement in the DFE is less significant, when compared to the linear equalizer. The filter taps in the DFE are adjusted most commonly to minimize the MSE at output. The DFE like the LE, can take the form of a zero forcing DFE. However, this may lead to noise enhancement so a better alternative and most common is the MSE-DFE. Although the problem of the noise enhancement is greatly reduced by the DFE, a serious degradation in the equalizer performance, known as error propagation phenomenon, appears. Whenever an erroneous decision is fed back into the feedback filter, the filter produces an output estimate, which is erroneous; this leads to another erroneous decision being fed back. In this way, error propagates and causes more errors in the feedback loop.

The sequence estimators constitute the second class of the equalizers and contain *maximum likelihood sequence estimator* and its suboptimum variants. Sequence estimator does not attempt to remove ISI terms from received signal. Instead, it estimates the transmitted sequence by searching the most likely transmitted symbols on the sequence of received signal samples. Maximum likelihood sequence estimation (MLSE) is an optimum algorithm for minimizing the probability of sequence error while symbol equalizers are suboptimum ones with respect to this criterion. Although it provides improved performance as compared to LE or DFE, its high computational complexity is its main drawback. The complexity of MLSE grows exponentially with the size of signal constellation, M , and length of channel memory, L as M^L . It can be a suitable equalization technique for the systems with low modulation size, i.e. GSM with modulation size of 2, even if transmitted signal is distorted with severe ISI. However, for systems with high values of signal alphabet, MLSE is impractical to implement with long channel memory. For example, if 8-PSK is used as modulation with channel impulse response of length 7 the algorithm complexity becomes order of 8^6 that is 262144.

The delayed decision feedback sequence estimation (DDFSE) [10][8] is a reduced-state sequence estimation algorithm, which decreases the computational complexity of the MLSE. It is a suboptimal algorithm and provides a tradeoff between performance and complexity by truncating the effective channel memory to μ terms, where μ is an integer that can be varied from 0 to the channel memory. By doing so, the complexity of the algorithm can be controlled with controlled degradation in performance with respect to MLSE. In this thesis, the DDFSE algorithm is chosen to perform the

equalization task for EGPRS and more detailed information is given in section 2.3.

2.2 Maximum Likelihood Sequence Estimation

The Maximum Likelihood Sequence Estimation (MLSE) is performed by computing the likelihoods for every possible transmitted sequence and by selecting the sequence with the largest likelihood. The likelihoods are obtained as the product of the probabilities of receiving each signal sample, given that particular transmitted sequence. Although the method is conceptually simple, the direct solution of this maximization problem is to test all possible input sequences. Instead of this direct approach, Forney [24] showed that the Viterbi algorithm provides the method for MLSE. The principle of the algorithm is to choose the path through the ISI trellis that has the minimum accumulated distance between the received data sequence corrupted by white-Gaussian noise and the hypothetical data sequences. The scheme is summarized in following lines [8].

MLSE algorithm searches, $\hat{\mathbf{x}}$ the estimate of transmitted vector \mathbf{x} , that maximize the likelihood function,

$$\hat{\mathbf{x}} = \max[p(\mathbf{r} | \mathbf{x}) = p(r_{N-1}, K, r_0 | x_{N-1}, K, x_0)] \quad (2-1)$$

where, N is the length of the transmitted sequence and r_k is received symbol at time k , which is defined as follows

$$r_k = \sum_{n=0}^L x_{k-n} h_n + z_k \quad (2-2)$$

h is the channel impulse response of the channel between transmitted symbols and received ones, L is channel memory, z_k 's are additive noise samples.

Since the additive noise is white gaussian, its samples are independent. Hence, the likelihood function in equation (2.1) corresponds to,

$$p(\mathbf{r} | \mathbf{x}) = \prod_{k=0}^{N-1} p(r_k | x_{N-1}, \mathbf{K}, x_0) \quad (2-3)$$

The log-likelihood function, therefore, is

$$\ln[p(\mathbf{r} | \mathbf{x})] = \sum_{k=0}^{N-1} \ln[p(r_k | x_{N-1}, \mathbf{K}, x_0)] \quad (2-4)$$

Since r_k depends only on the L most recent transmitted symbols, the log-likelihood function can be rewritten as

$$\ln[p(\mathbf{r} | \mathbf{x})] = \ln[p(r_{N-1} | x_{N-1}, \mathbf{K}, x_{N-1-L})] + \ln[p(r_{N-2}, \mathbf{K}, r_0 | x_{N-2}, \mathbf{K}, x_0)] \quad (2-5)$$

If the second term on the right hand side of equation has been calculated previously at epoch $N-2$, then only the first term, called the *branch metric*, has to be computed for incoming signal sample, r_{N-1} at epoch $N-1$. With the

well-known equality (2.6) for $p(r_k | x_k, \mathbf{K}, x_{k-L})$ with r_k in equation (2.5), branch metric at time k , μ_k , yields equation (2.7) [7]

$$p(r_k | x_k, \mathbf{K}, x_{k-L}) = \frac{1}{\sqrt{2\pi}\sigma^2} \exp \left\{ -\frac{1}{2\sigma^2} \left| r_k - \sum_{i=0}^L h_i x_{k-i} \right|^2 \right\} \quad (2-6)$$

$$\mu_k = -\left| r_k - \sum_{i=0}^L h_i x_{k-i} \right|^2 \quad (2-7)$$

where σ^2 is variance of additive white gaussian noise.

Based on the recursion in equation (2.5) and the branch metric in equation (2.7), the well-known Viterbi algorithm can be used to determine the most likely transmitted sequence.

2.3 Delayed Decision-Feedback Sequence Estimation (DDFSE)

Unfortunately, the complexity of the MLSE receiver grows exponentially with the channel memory length and symbol alphabet. When the channel memory length becomes large, the MLSE receiver is impractical. One solution is to reduce the receiver complexity by truncating the effective channel memory to μ terms, where μ is an integer that can be varied from 0 to L . Thus, a suboptimum decoder is obtained with complexity controlled by parameter μ . This is the basic idea for Delayed Decision Sequence Estimation (DDFSE) [10][8]. The DDFSE receiver can be viewed as combination of the MLSE operating on received samples and the decision feedback that works like a detector.

In maximum likelihood sequence estimation, when the vector r_k has been received, the Viterbi algorithm searches through the $S = M^L$ state trellis for the most likely transmitted sequence \mathbf{x} . The state $s_k^{(j)}$ for $j = 0, \dots, S-1$ is built with state sequence $s_k = (x_{k-1}, \mathbf{K}, x_{k-L})$. In the DDFSE, this sequence is decomposed into the state $s_k^\mu = (x_{k-1}, \mathbf{K}, x_{k-\mu})$ and the associated partial state $v_k = (x_{k-\mu-1}, \mathbf{K}, x_{k-L})$. And the received symbols are considered as decomposition of the μ recents symbols and the symbols transmitted from time $\mu-1$ to L ;

$$r_k = \sum_{i=0}^{\mu} h_i x_{k-i} + w_k + z_k \quad (2-8)$$

where w_k is partial state metric and defined with partial state sequence as

$$w_k = \sum_{i=\mu+1}^L h_i x_{k-i} \quad (2-9)$$

Then, the DDFSE algorithm is implemented by the viterbi algorithm with the state sequence s_k^μ , therefore with $S_{DDFSE} = M^\mu$ states. For each state transition $s_k^{\mu(i)} \rightarrow s_{k+1}^{\mu(j)}$, the DDFSE stores S_{DDFSE} estimates of partial state v_k associated with each state at time k . The algorithm can be summarized as follows:

For each state $s_{k+1}^{\mu(j)}$ for $j = 0, \dots, M^\mu - 1$

1. Compute the set of path metrics

$$\Gamma(s_k^{\mu(i)} \rightarrow s_{k+1}^{\mu(j)}) = \Gamma(s_k^{\mu(i)}) + \mu(s_k^{\mu(i)} \rightarrow s_{k+1}^{\mu(j)})$$

for all possible paths through the trellis that terminate in state $s_{k+1}^{\mu(j)}$.

$\mu(s_k^{\mu(i)} \rightarrow s_{k+1}^{\mu(j)})$ is the branch metric associated with the transition $s_k^{\mu(i)} \rightarrow s_{k+1}^{\mu(j)}$ and is computed according to the following of equation

$$\mu(s_k^{\mu(i)} \rightarrow s_{k+1}^{\mu(j)}) = - \left| r_k - h_0 x_k(s_k^{\mu(i)} \rightarrow s_{k+1}^{\mu(j)}) - \sum_{l=1}^{\mu} h_l x_{k-l}(s_k^{\mu(i)}) + \hat{w} \right|^2 \quad (2-10)$$

where $x_k(s_k^{\mu(i)} \rightarrow s_{k+1}^{\mu(j)})$ is symbol that is determined by the transition $s_k^{\mu(i)} \rightarrow s_{k+1}^{\mu(j)}$, \hat{w} is the partial state metric of the state $s_k^{\mu(i)}$.

2. Find $\Gamma(s_{k+1}^{\mu(j)}) = \max \Gamma(s_k^{\mu(i)} \rightarrow s_{k+1}^{\mu(j)})$ where the maximization is over all possible paths through the trellis that terminate in state $s_{k+1}^{\mu(j)}$.
3. Store $\Gamma(s_{k+1}^{\mu(j)})$ and its associated surviving state. Drop all other paths.
4. Build partial state $v_{k+1} = (x_{k-\mu}, K, x_{k+1-L})$ using the partial state of the surviving state and the symbol estimated at the state transition.

After all states have been processed, the time index k is incremented and the whole algorithm repeats. At the end, i.e. $k = N-1$, the surviving paths are traced back to find the estimates of the transmitted sequence as in MLSE.

The algorithm can be summarized in figure (2.1) for binary case with $L = 4$ and $\mu=2$;

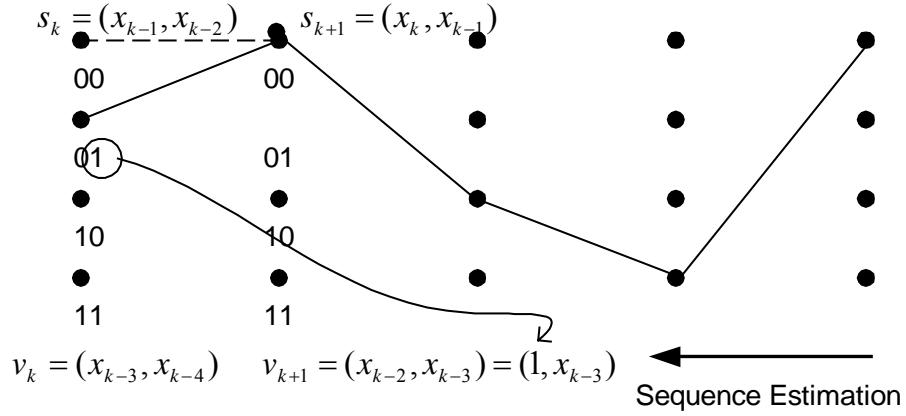


Figure 2.1. DDFSE algorithm for binary case with $L = 4$ and $\mu = 2$

In figure (2.1), the state with state sequence $(x_{k-1}, x_{k-2}) = (0, 1)$ is investigated as surviving state by computing two possible path metrics of the paths terminated at state s_{k+1} and then, performing maximization operation over the path metrics. After determining surviving state, partial state $v_{k+1} = (x_{k-2}, x_{k-3})$ is built as shown in figure (2.1) using the partial state of the surviving state, $v_k = (x_{k-3}, x_{k-4})$, and the symbol estimated at the state transition $s_k \rightarrow s_{k+1}$, x_{k-2} .

Since only the μ most recent symbols are represented in the trellis structure, it is important to have most of the signal energy contained in these terms. Hence, in order to obtain high performance, the channel impulse response seen by equalizer should have minimum phase characteristics. Therefore, a prefiltering, in the front of equalization is performed to transform channel impulse response into its minimum phase equivalent. Prefilter design is considered in section 4.3.2.

2.4 Computational Complexity Comparison of MLSE and DDFSE Algorithms

In order to obtain a meaningful comparison between the computational complexity of the MLSE and the DDFSE algorithms, a guide to the computational complexity is derived here. The analysis is due to the implementation of the algorithms performed in this thesis. In any real implementation, complex algorithms may be further optimized and shortcuts taken. The figures for complexity in the following lines therefore are indicative only. Computations are for baseband processing in the receiver and assume a single sample/symbol.

Consider the MLSE and the DDFSE algorithms applied to symbols constellation with M components and transmitted through a channel with L taps. The number of states in the trellis is given by $S_{MLSE} = M^L$ for MLSE and by $S_{DDFSE} = M^\mu$ for DDFSE.

The MLSE algorithm consists of the following significant stages

1. State sequences for all possible states are convolved with ISI terms in CIR and stored initially. This requires LS_{MLSE} multiplication and additions. This step needs only be performed when a new sampled channel impulse response is computed.
2. For each state transition, the branch metric in equation (2.7) is calculated with 2 additions and 2 multiplication, and 1 more addition is needed to determine the path metric. Since each state is connected to M states, This step requires $3MS_{MLSE}$ addition and $2MS_{MLSE}$ multiplication.

3. For each state, the surviving path is determined by choosing a survivor among the M states connected to processing state, which results in MS_{MLSE} comparison operations.

If the same analysis is performed for DDFSE algorithm, the following results are obtained for each stage;

1. The initial metrics are computed with LS_{DDFSE} multiplication and additions: μS_{DDFSE} of the total number of operations is required for trellis structure and $(L - \mu)S_{DDFSE}$ multiplication and additions are for partial state metrics since each path has own path history.
2. Computation of the surviving path metric requires $4MS_{DDFSE}$ additions and $2MS_{DDFSE}$ multiplication. The additional MS_{DDFSE} additions with respect to MLSE case are performed to add partial state metrics in computing the branch metric (2.10), which is not considered in the case $\mu = L$.
3. For each state, a survivor is chosen among the M states connected to processing state resulting MS_{DDFSE} comparison operations in the algorithm.

The computational complexities of the MLSE and the DDFSE algorithms based on the addition (ADD), multiplication (MULTIP) and comparison (COMP) operations are given in table 2.1 and in table 2.2 for some specific values of channel memory and constellation size. Since the first steps expressed above needs only are performed when the CIR changes and so is

not necessarily computed every symbol period, it is considered as initial in separate columns of the tables.

Table 2.1. Computational Complexity of the MLSE and the DDFSE algorithms

	Operation/Symbol			Initial	
	ADD	MULTIP	COMP	ADD	MULTIP
MLSE	$3MM^L$	$2MM^L$	MM^L	LM^L	LM^L
DDFSE	$4MM^\mu$	$2MM^\mu$	MM^μ	LM^μ	LM^μ

Table 2.2. Computational Complexity of the MLSE and The DDFSE algorithms for specific vales

Truncated Channel Memory μ	Modulation Index							
	$M=2$				$M=8$			
	Operation/Symbol			Initial	Operation/Symbol			Initial
	ADD	MULTIP	COMP	ADD /MULTIP	ADD	MULTIP	COMP	ADD /MULTIP
DDFSE 2	32	16	8	28	2048	1024	512	448
4	128	64	32	112	131072	65536	32768	28672
6	512	256	128	448	8.3×10^6	4.2×10^6	2.1×10^6	1.8×10^6
MLSE 7	768	512	256	896	5.0×10^7	3.3×10^7	1.6×10^7	1.4×10^7

CHAPTER 3

TURBO EQUALIZATION

Channel coding and interleaving techniques has long been recognized as an effective technique for combating the effects of noise, interference and other channel impairments. The basic idea of channel coding is to introduce controlled redundancy into the transmitted signals that is exploited at the receiver to correct channel induced errors by means of forward error correction. Significant improvements in bit error rate (BER) performance are possible by coded data transmission using channel coding. At the receiver part of such systems, an equalizer to accommodate ISI, and a decoder that uses information provided by equalizer are required to obtain information sequence being coded. The decoder is fed either with hard information (symbol estimates only) or soft information. Communicating soft information between the equalizer and the decoder, instead of hard information, improves bit error rate generally, since soft information has more reliable information.

The recent systems for a variety of communication channels employ an interleaver with convolutional codes. This is due to the fact that convolutional codes are designed to combat randomly distributed, statistically independent errors. In order to achieve robust error correction on

channels having memory, interleaving combined with convolutional coding constitutes an appropriate means. The interleaver maps the coded sequence one-to-one to the output sequence by rearranging the order of the symbols. At the receiver, the demodulated symbol estimates are correlated. The deinterleaver, carrying out the reverse process of the interleaver, decorrelates the relative positions of the symbols respectively in the demodulator output and in the decoder input. Error bursts are rearranged to single errors or at least to smaller length errors. Due to interleaving, the decoder can decode the statistically independent data better.

Conventional receivers generally perform equalization and channel coding separately. In 1995, Douillard et al pioneered a joint iterative channel equalization and decoding technique [12], whereby the channel decoder is utilized in order to improve the performance of the equalization process and vice versa in an iterative regime. This scheme, called as Turbo Detection², combines a soft-in/soft-out (SISO) detector with a soft-in/soft-out (SISO) decoder through an iterative process.

3.1 *Turbo Principle*

The turbo principle was first applied to iteratively decode parallelly concatenated recursive systematic codes. Viewing the linear channel as a

² In some references in the literature, Turbo Detection is also called as Turbo Equalization. However, in some other references Turbo detection refers to the iterative scheme, which employs trellis, based algorithms in SISO equalization while the scheme is named as Turbo Equalization if a reduced complexity equalization, decision feedback or linear equalization, is used.

convolutional encoder, the turbo principle is applied to channel equalization in conjunction with error correcting decoder in [12] and adapted to mobile communication systems in [14].

The components of a turbo detector are the soft-in/soft-out (SISO) detector and the soft-in/soft-out SISO decoder, which feed each other with soft decision values iteratively. The soft values exchanged between equalizer and decoder are in the form of log-likelihood ratios and called as L-values:

$$L(c_k) = \ln \frac{p(c_k = 1 | \mathbf{r})}{p(c_k = -1 | \mathbf{r})} \quad (3-1)$$

where c_k is the k^{th} bit of the coded bit sequence \mathbf{c} .

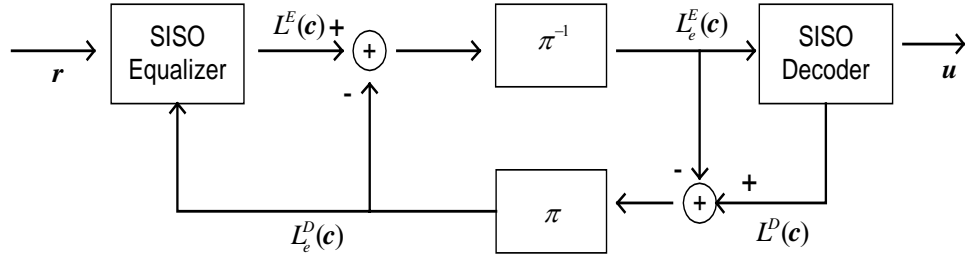


Figure 3. 1. Turbo Detection Scheme

In figure (3.1), the scheme of iterative detection and decoding is depicted. For each iteration, the SISO equalizer obtains the received symbol values \mathbf{r} and equalizes them by providing soft values (L-values) about coded bit

sequence, $L^E(\mathbf{c})$. The L-values of the coded sequence \mathbf{c} has two components: The intrinsic part and the extrinsic part. The extrinsic part represents the incremental information generated by the equalizer with the information available from all other bits. The soft value fed back to the decoder is the extrinsic part of the L-values. As can be seen from the figure (3.1), the information generated by the decoder at the previous iteration, $L_e^D(\mathbf{c})$, represent the intrinsic part and the extrinsic part is obtained by subtracting this intrinsic information from the L-values produced by the equalizer, $L^E(\mathbf{c})$. Then, this information is deinterleaved to place the extrinsic L-values into the correct order to build $L_e^E(\mathbf{c})$, a priori value fed to the decoder

$$L_e^E(\mathbf{c}) = \pi^{-1}(L^E(\mathbf{c}) - L_e^D(\mathbf{c}))$$

where π^{-1} represent deinterleaving operation.

The only exception in this process appears in the 0th iteration. At that time, since there is no L-value available from the decoder, a priori information for the equalizer is set to zero, i.e., $L_e^D(\mathbf{c}) = 0$ and, the L-values delivered by the equalizer, $L^E(\mathbf{c})$, is deinterleaved without no information extracted.

The SISO decoder uses deinterleaved extrinsic L-values from the equalizer as a priori information, $L_e^E(\mathbf{c})$, to generate the L-values about the information sequence \mathbf{u} , $L^D(\mathbf{u})$, and the L-values about the coded sequence \mathbf{c} , $L^D(\mathbf{c})$. The L-values of information sequence is, generally, not used in the iterative process, it is required to determine the hard estimates of information sequence \mathbf{u} as follows;

$$u_k = \begin{cases} 1 & L^D(u_k) \geq 0 \\ 0 & L^D(u_k) < 0 \end{cases} \quad (3-2)$$

But L-values of the coded sequence, $L^D(\mathbf{c})$ is fed back to the equalizer by subtracting a priori values of the decoder, $L_e^E(\mathbf{c})$ representing the intrinsic part. This information is interleaved to place the values into the correct order for the equalizer. The information at the input of the equalizer is defined as follows

$$L_e^D(\mathbf{c}) = \pi(L^D(\mathbf{c}) - L_e^E(\mathbf{c}))$$

where π represent interleaving operation.

In order to improve the bit error rate performance, the same procedure is repeated using the L-values from the decoder for equalization and L-values from the equalizer for decoder. By this iterative process, the equalizer can generate a more accurate output with the additional information from the decoder, $L_e^D(\mathbf{c})$, and the decoder can improve the bit error rate by using the improved estimates of the equalizer, $L_e^E(\mathbf{c})$. It is essential to turbo detection that the decoder/equalizer does not pass the information to the equalizer/decoder that was generated by the decoder/equalizer at the previous iteration. If the a priori information is not removed from the L-values, the iteration gains decrease significantly; the L-values passed between the components become too optimistic.

From [12], it is known that the iteration gain of the first iteration is the largest. The iteration gains decrease from iteration to iteration until the bit error rate performance converges. There are several strategies to limit the

number of iterations, such as stop criteria. In [29], some stop criteria, which adaptively decide when iterations are stopped, have been evaluated. The authors showed that by adaptively determining the number of the iterations for each block, the complexity the decoder could be reduced. In practical systems, a fixed number of iterations can be accommodated with a trade of between number of iterations and hardware cost.

3.2 SISO Decoding/Equalization

SISO equalization and decoding are critical parts of the turbo equalization since the performance of turbo-scheme strongly depends on the quality of the soft values passed between the soft-in/soft-out decoder and equalizer. As already mentioned, they get a priori probabilities in the form of log-likelihood ratio about the coded sequence \mathbf{c} , and generate a posteriori probabilities about coded sequence, and about information sequence, \mathbf{u} , in the same form.

Optimum soft information required by detection and decoding can be produced by the symbol-by-symbol maximum a posteriori (MAP) decoding algorithm. To accomplish this task, the BCJR³ MAP [13] algorithm is utilized in this thesis since it is considered to be the least complex and more suitable algorithm for block transmission [14][15]. The MAP algorithm refers to the BCJR MAP from now on.

³ Due to the initials of [13]'s authors. It is also referred to as Bahl algorithm.

3.2.1 MAP Decoding Algorithms

MAP algorithm is a trellis-based algorithm, and it delivers the a posteriori probabilities (APP) of the desired sequence by computing transition probabilities of each state. The log-likelihood ratios, therefore, can be obtained using the a posteriori probabilities.

Let the input sequence of algorithm be $\mathbf{r} = \{r_0, \dots, r_{N-1}\}$ and the sequence whose log-likelihood ratios will be estimated is $\mathbf{m} = \{m_0, \dots, m_{N-1}\}$. As will be seen in following sections, m_k represents either a information bit (in decoding process) or a symbol value (in equalization part).

The MAP algorithm defines three quantities to find the a posteriori probabilities for \mathbf{m} :

The *forward probability* which is defined as the joint probability of state $s_k^{(i)}$ at time k and input sequence \mathbf{r} from time 0 to $k-1$.

$$\alpha(s_k^{(i)}) = p(s_k^{(i)}, (r_0, \dots, r_{k-1})) \quad (3-3)$$

The *backward probability* as the probability of the input sequence from time k to $N-1$, under the condition of state $s_k^{(i)}$ at time k .

$$\beta(s_k^{(i)}) = p((r_k, \dots, r_{N-1}) | s_k^{(i)}) \quad (3-4)$$

The *branch transition probability* as the joint probability of state $s_k^{(i)}$ at time k , and the input value r_k under the condition of state $s_{k-1}^{(j)}$ at time $k-1$.

$$\mu(s_k^{(j)} \rightarrow s_{k+1}^{(i)}) = p(s_{k+1}^{(i)}, r_k | s_k^{(j)}) \quad (3-5)$$

Then the APP for message bit m_k are determined as

$$\begin{aligned} p(m_k = 1 | \mathbf{r}) &= \left(\sum_{S_0} \alpha(s_k^{(j)}) \mu(s_k^{(j)} \rightarrow s_{k+1}^{(i)}) \beta(s_{k+1}^{(i)}) \right) / p(\mathbf{r}) \\ p(m_k = 0 | \mathbf{r}) &= \left(\sum_{S_0} \alpha(s_k^{(j)}) \mu(s_k^{(j)} \rightarrow s_{k+1}^{(i)}) \beta(s_{k+1}^{(i)}) \right) / p(\mathbf{r}) \end{aligned} \quad (3-6)$$

where $S_1 = (s_k^{(j)} \rightarrow s_{k+1}^{(i)} | m_k = 1)$ is the all state transitions associated with 1 and $S_0 = (s_k^{(j)} \rightarrow s_{k+1}^{(i)} | m_k = 0)$ is the all state transitions associated with 0. Then, log-likelihood ratios are obtained as

$$L(m_k) = \ln \frac{\sum_{S_1} \alpha(s_k^{(j)}) \mu(s_k^{(j)} \rightarrow s_{k+1}^{(i)}) \beta(s_{k+1}^{(i)})}{\sum_{S_0} \alpha(s_k^{(j)}) \mu(s_k^{(j)} \rightarrow s_{k+1}^{(i)}) \beta(s_{k+1}^{(i)})} \quad (3-7)$$

The forward probability can be found according to the following recursion:

$$\alpha(s_k^{(i)}) = \sum_{s_{k-1}^{(j)} \in A} \alpha(s_{k-1}^{(j)}) \mu(s_{k-1}^{(j)} \rightarrow s_k^{(i)}) \quad (3-8)$$

where A is the set of states $s_{k-1}^{(j)}$ that are connected to state $s_k^{(i)}$.

Likewise $\beta(s_k^{(i)})$ can be found using the following recursion:

$$\beta(s_k^{(i)}) = \sum_{s_{k+1}^{(j)} \in B} \beta(s_{k+1}^{(j)}) \mu(s_k^{(i)} \rightarrow s_{k+1}^{(j)}) \quad (3-9)$$

where B is the set of state $s_{k+1}^{(j)}$ that are connected to state $s_k^{(i)}$.

If trellis states stay at state $s_0^{(initial)}$ at the beginning and terminate at final state $s_N^{(final)}$ at the end, initializations of backward and forward probabilities are as follows:

$$\alpha(s_0^{(i)}) = \begin{cases} 1 & i = initial \\ 0 & i \neq initial \end{cases} \quad (3-10)$$

$$\beta(s_N^{(i)}) = \begin{cases} 1 & i = final \\ 0 & i \neq final \end{cases}$$

If the trellis is not terminated, states are equally probable and initial backward probability can be determined as

$$\beta(s_N^{(i)}) = \frac{1}{M^L} \quad \forall i \quad (3-11)$$

where M is 2 for the binary case and $L+1$ is the length of channel impulse response.

Although the MAP algorithm is able to calculate precise estimates the a posteriori probability of each information bit, it suffers from high

computational complexity. The calculations can be simplified and numerical stability can be improved by performing the calculations in the logarithmic domain, resulting in the log-MAP algorithm. The log-MAP algorithm is still optimum with respect to bit error probability and generates the same a posteriori values as the symbol-by-symbol MAP algorithm.

In the case of log-MAP algorithm, Log-likelihood ratios are defined in following equation

$$L(m_k) = \ln \sum_{S_1} e^{\ln[\alpha(s_k^{(j)})] + \ln[\mu(s_k^{(j)} \rightarrow s_{k+1}^{(i)})] + \ln[\beta(s_{k+1}^{(i)})]} - \ln \sum_{S_0} e^{\ln[\alpha(s_k^{(j)})] + \ln[\mu(s_k^{(j)} \rightarrow s_{k+1}^{(i)})] + \ln[\beta(s_{k+1}^{(i)})]} \quad (3-12)$$

where

$$\begin{aligned} \ln[\alpha(s_k^{(i)})] &= \ln \sum_{s_{k-1}^{(j)} \in A} e^{\ln[\alpha(s_{k-1}^{(j)})] + \ln[\mu(s_{k-1}^{(j)} \rightarrow s_k^{(i)})]} \\ \ln[\beta(s_k^{(i)})] &= \ln \sum_{s_{k+1}^{(j)} \in B} e^{\ln[\beta(s_{k+1}^{(j)})] + \ln[\mu(s_k^{(i)} \rightarrow s_{k+1}^{(j)})]} \end{aligned} \quad (3-13)$$

with the following initial probabilities

$$\begin{aligned} \ln[\alpha(s_0^{(i)})] &= \begin{cases} 0 & i = \text{initial} \\ -\infty & i \neq \text{initial} \end{cases} \\ \ln[\beta(s_N^{(i)})] &= \begin{cases} 0 & i = \text{final} \\ -\infty & i \neq \text{final} \end{cases} \end{aligned} \quad (3-14)$$

Although the log-MAP simplifies the implementation of the MAP algorithm, computational complexity is still high. It can be reduced by a sub-optimal Max-log-MAP algorithm, which is derived from the log-MAP algorithm by invoking the so-called Jacobian logarithm relation.

$$\begin{aligned}
J(x_1 + x_2) &= \ln(e^{x_1} + e^{x_2}) = \max(x_1, x_2) + \ln(1 + e^{-|x_1 - x_2|}) \\
&= \max(x_1, x_2) + f_c(|x_1 - x_2|) \\
&\approx \max(x_1, x_2)
\end{aligned} \tag{3-15}$$

For the case where the states are connected more than two state in the trellis, corresponding to non-binary case, the Jacobian logarithmic relation in equation (3.15) can be extended to cope with a higher number of exponential summations. Reference [31] shows that this can be achieved by nesting the

$$\ln \sum_{k=1}^n e^{x_k} \text{ operation as } \ln \sum_{k=1}^n e^{x_k} = J(x_n, J(x_{n-1}, K J(x_3, J(x_2, x_1)) K)).$$

$f_c(x)$ in (3.15) is the error function and its value is negligible for $x \ll y$ and $y \ll x$ and is in the worst case $\ln 2$ for $x = y$. From the simulations it turns out that this approximation has only a slight effect on the overall performance of the conventional receiver structure [30] and of the turbo detection if the receiver does not have ideal channel knowledge [14].

Using the approximation in (3.15), forward transition probability of a state at time k is computed with maximization operator over all states at time $k-1$, which are connected to that state, instead of adding corresponding transition probabilities up as in MAP and log-MAP case. The same simplification

procedure can be performed for backward transition probabilities using maximization operation as follows:

$$\begin{aligned}\bar{\alpha}(s_k^{(i)}) &= \ln[\alpha(s_k^{(i)})] = \ln \sum_{s_{k-1}^{(j)} \in A} e^{[\bar{\alpha}(s_{k-1}^{(j)}) + \bar{\mu}(s_{k-1}^{(j)} \rightarrow s_k^{(i)})]} \\ &= \max_{s_{k-1}^{(j)} \in A} [\bar{\alpha}(s_{k-1}^{(j)}) + \bar{\mu}(s_{k-1}^{(j)} \rightarrow s_k^{(i)})]\end{aligned}\tag{3-16}$$

$$\begin{aligned}\bar{\beta}(s_k^{(i)}) &= \ln[\beta(s_k^{(i)})] = \ln \sum_{s_{k+1}^{(j)} \in B} e^{[\bar{\beta}(s_{k+1}^{(j)}) + \bar{\mu}(s_k^{(i)} \rightarrow s_{k+1}^{(j)})]} \\ &= \max_{s_{k+1}^{(j)} \in B} [\bar{\beta}(s_{k+1}^{(j)}) + \bar{\mu}(s_k^{(i)} \rightarrow s_{k+1}^{(j)})]\end{aligned}$$

The Log-likelihood ratios for m_k are therefore computed by the following simplified equation:

$$\begin{aligned}L(m_k) &= \max_{S_1} [\bar{\alpha}(s_k^{(j)}) + \bar{\mu}(s_k^{(j)} \rightarrow s_{k+1}^{(i)}) + \bar{\beta}(s_{k+1}^{(i)})] \\ &\quad - \max_{S_0} [\bar{\alpha}(s_k^{(j)}) + \bar{\mu}(s_k^{(j)} \rightarrow s_{k+1}^{(i)}) + \bar{\beta}(s_{k+1}^{(i)})]\end{aligned}\tag{3-17}$$

3.2.2 SISO Decoder

The SISO decoder can use one of the MAP algorithms to generate a posteriori information (L-values) about the information sequence $L^D(\mathbf{u})$ and about coded bits $L^D(\mathbf{c})$ using a priori information, deinterleaved extrinsic L-values, from the SISO equalizer, $L_e^E(\mathbf{c})$.

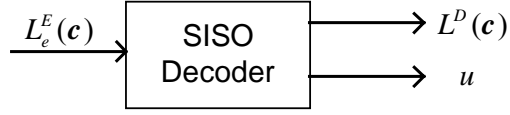


Figure 3. 2. SISO decoder

The trellis structure is built with 2^{K-1} states where state sequence at time k is $s_k = (u_{k-1}, \dots, u_{k-K+1})$ and K is the constraint length of the encoder (see figure 3.3).

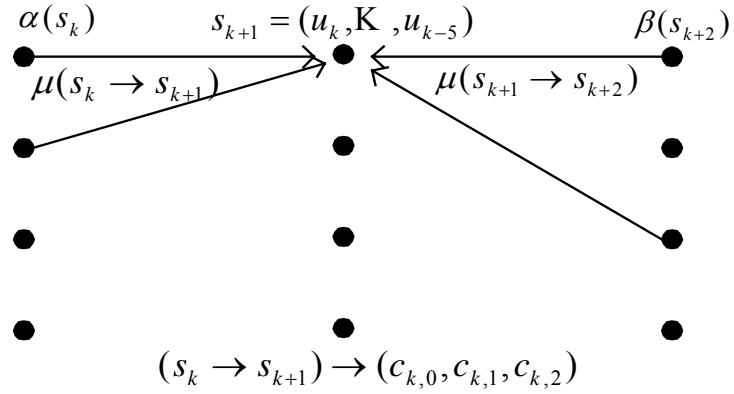


Figure 3.3. Structure of MAP algorithm for SISO decoder, $K=7$ and coding rate $1/3$

For each state at time k , backward transition and forward transition probabilities are computed with equation (3.16) by utilizing L-values from the equalizer in the branch transition probability as like:

$$\bar{\mu}(s_k \rightarrow s_{k+1}) = \sum_{i=1}^N L_e^E(c_{k,i}) c_{k,i} \quad (3-18)$$

where $c_{k,i}$ is the i^{th} code bit for information bit u_k , and $1/N$ is the coding rate.

Then, the L-values of SISO decoder for information sequence \mathbf{u} are evaluated using the expression defined in expression (3.17) as follows

$$\begin{aligned} L(u_k) = & \max_{\substack{(s_k^{(j)}, s_{k+1}^{(i)}) \\ u_k=+1}} \left\{ \bar{\alpha}(s_k^{(j)}) + \bar{\mu}(s_k^{(j)} \rightarrow s_{k+1}^{(i)}) + \bar{\beta}(s_{k+1}^{(i)}) \right\} \\ & - \max_{\substack{(s_k^{(j)}, s_{k+1}^{(i)}) \\ u_k=-1}} \left\{ \bar{\alpha}(s_k^{(j)}) + \bar{\mu}(s_k^{(j)} \rightarrow s_{k+1}^{(i)}) + \bar{\beta}(s_{k+1}^{(i)}) \right\} \end{aligned} \quad (3-19)$$

Since state transition $s_k^{(j)} \rightarrow s_{k+1}^{(i)}$ determines code bits $c_{k,i}$ $i=1, \dots, N$, L-value for each code bit can be obtained as;

$$\begin{aligned} L(c_{k,i}) = & \max_{\substack{(s_k^{(j)}, s_{k+1}^{(i)}) \\ c_{k,i}=+1}} \left\{ \bar{\alpha}(s_k^{(j)}) + \bar{\mu}(s_k^{(j)} \rightarrow s_{k+1}^{(i)}) + \bar{\beta}(s_{k+1}^{(i)}) \right\} \\ & - \max_{\substack{(s_k^{(j)}, s_{k+1}^{(i)}) \\ c_{k,i}=-1}} \left\{ \bar{\alpha}(s_k^{(j)}) + \bar{\mu}(s_k^{(j)} \rightarrow s_{k+1}^{(i)}) + \bar{\beta}(s_{k+1}^{(i)}) \right\} \end{aligned} \quad (3-20)$$

Note that L-values given equation (3.19) and equation (3.20) are for Max-Log-MAP algorithm. But L-values for the log-MAP and the MAP algorithms can be determined likewise by using equation (3.8)-(3.9) and equation (3.12) with transition probability in equation (3.18).

3.2.3 SISO Equalizer

The SISO equalizer should produce L-values for coded bits under the condition of received symbols from transmission channel and L-values from decoder.



Figure 3. 4. SISO equalizer

For this purpose, SISO equalizer employs a MAP algorithm by utilizing a priori information from decoder in the transition probability as incremental information. However since the equalizer is working symbol-wise, L-values from decoder about coded bits $L_e^D(c)$ should be adopted to L-values about symbols values $L_e^D(x)$ to employ L-values from the decoder in the transition probability. Similar to the binary case, the log-likelihood ratios are obtained by comparing the probability of certain symbol to the probability of a reference symbol, e.g. in binary case the probability of -1 is compared to the probability of 1, as in equation (3.1). Reference symbol can be taken as the symbol corresponding to the $ld(M)$ -tuple minus ones [15]. In this way, with $x_k(i)$ being the i^{th} bit of the tuple corresponding to the symbol x_k , the symbol L-value is defined as follows:

$$\begin{aligned}
L_e^D(x_k) &= \ln \frac{\prod_{i=1}^{ld(M)} p(c_{k,i} = x_k(i))}{\prod_{i=1}^{ld(M)} p(c_{k,i} = -1)} \\
&= \sum_{\substack{i=1 \\ x_k(i)=+1}}^{ld(M)} L(c_{k,i})
\end{aligned} \tag{3-18}$$

with M being the size of symbol alphabet and $j \in \{1, \dots, M\}$ and $c_{k,i} = c_{k + ld(M) \times i}$.

Therefore, the symbol L-value is obtained by adding the bit L-values from the decoder for those bits of the symbol x_k that are equal to 1.

Example 3.1 : The symbol space of 8-PSK modulation is built with 3-tuples of the symbols. Considering equation (3.22), the relation between the symbol L-value $L_e^D(x_k)$ and bit L-value $L_e^D(c_{k,i})$ for the symbol represented by the 3-tuples of (1,-1,1) is given by $L_e^D(x_k) = L_e^D(c_{k,1}) + L_e^D(c_{k,3})$.

With this definition of the symbol L-values, transition probability of a MAP algorithm is given as

$$\bar{\mu}(s_k^{(j)} \rightarrow s_{k+1}^{(i)}) = -\frac{1}{2\sigma^2} \left| r_k - \sum_{i=0}^L h_i x_{k-i} \right|^2 + L_e^D(x_k) \tag{3-18}$$

where r_k is the received symbol (equation 2.2) and \mathbf{h} is channel impulse response with length L .

Using the transition probability in equation (3.21), the backward and the forward transition probabilities can be computed with equation (3.16), i.e. for log-Max-MAP case, for each state in the trellis structure built by state sequence $s_k = (x_{k-1}, \dots, x_{k-L})$.

After applying backward and forward trellis search, L-values about coded bits are obtained with following equation, i.e. for Max-Log case.

$$L(c_k) = \max_{\substack{(s_k^{(j)}, s_{k+1}^{(i)}) \\ x_k(i)=1}} \{ \overline{\alpha}(s_k^{(j)}) + \overline{\mu}(s_k^{(j)} \rightarrow s_{k+1}^{(i)}) + \overline{\beta}(s_{k+1}^{(i)}) \} \\ - \max_{\substack{(s_k^{(j)}, s_{k+1}^{(i)}) \\ x_k(i)=-1}} \{ \overline{\alpha}(s_k^{(j)}) + \overline{\mu}(s_k^{(j)} \rightarrow s_{k+1}^{(i)}) + \overline{\beta}(s_{k+1}^{(i)}) \} \quad (3-19)$$

Difficulty of processing the large number of states often arises in equalization, when multilevel modulation is considered rather than binary ones. In this case, the complexity grows exponentially as modulation level and channel length grows as in MLSE. To overcome this problem of a trellis-based detector, the DDFSE can be utilized in a MAP algorithm to perform a reduced-state detection [31][26][33][34][36]. This type of detector applies the MAP algorithm in a trellis structure whose states are reduced by the DDFSE principle defined in section 2.3. The details of this type of detector can be found in section 4.3.3.

CHAPTER 4

EQUALIZATION AND TURBO DETECTION FOR EGPRS

EDGE can be seen as a generic air interface for efficiently increasing throughput of existing GSM 2+ systems HSCSD and GPRS by new modulation schemes and more powerful link quality control functions. Although EDGE supports both circuit switched (CS) and packet switched (PS) mode of operation, known as ECSD and EGPRS, the explosive growth of the Internet and the subsequent demand for wireless data communication have lead to packet switched services being a major component of mobile radio systems [4] and the term EDGE is frequently used as synonym of EGPRS [1].

One fundamental characteristic of a cellular system is that different users tend to have different channel due to difference in distance from base station, fading, and interference. In order to establish a reliable link between user and network with high data rate, powerful Link quality control techniques are introduced with EGPRS [27]. Link quality control is a common term for techniques to adapt the robustness of the radio link to varying channel

quality. Link quality control techniques EGPRS supports are a combination of *link adaptation* and *incremental redundancy*.

Link adaptation regularly estimates the link quality and subsequently selects the most appropriate modulation and coding scheme for coming transmissions in order to maximize the user bit rate related to channel quality [5],[6]. EGPRS has nine Modulation Coding Schemes (MCS) as expressed in section 4.1 to establish a sophisticated Link Adaptation.

In Incremental Redundancy, information with high coding rate is first sent, yielding a high bit rate if decoding is immediately successful. If decoding fails a retransmission is formed using a different puncturing scheme. The retransmission is combined with the previously received block to facilitate decoding. If initial transmission with high code rate fails and the quality of the radio channel diminishes, the retransmission can use more robust coding scheme [6]. Different code rates in EGRPS are achieved with puncturing convolutionally encoded information bits and for each Modulation Coding Scheme (MCS) is puncturing with different puncturing pattern.

After a suitable MCS is selected for optimal bit rates, data is transmitted over the air interface. Many EGPRS physical layer parameters are identical to those of GSM. The main difference is the modulation scheme; EGPRS applies the modulation format 8 PSK in conjunction with GMSK, which is already used in GSM. The carrier spacing is 200 kHz, and TDMA time slot structure of GSM is unchanged. Certain number of carriers, ranging from 1 to usually not more than 15 are assigned to individual base station. Time Division Multiple Access (TDMA) is used to segment the assign spectrum of 200 kHz per radio channel into 8 time slots of 0.577 ms. Each of the 8 time

slots is assigned to an individual user. The slots numbered from slot 0 to 7 form a frame with length 4.615 ms and all the users of a single frequency share a common frame. The recurrence of one particular time slot in each frame makes up a physical channel [17]. The physical channels are used to carry user and signaling or control information in the form of a burst, which is transmission quantum of GSM, and EGPRS. Different burst structures are defined related to type of data exchanged. Normal burst, as shown figure 4.1, is the most frequently used type, which is formed for all user data and some control messages. A normal burst contains two packets of 58 data symbols, each of whose comprising 3 bits for 8 PSK modulation, surrounding a training sequence of 26 symbols. The 26-symbol training sequence is of a known pattern, and it is compared with the received pattern in order to reconstruct the transmitted signal. Three “tail” bits are added on each side of burst structure. “Guard period” is actually considered as a defined time rather than actual data bits. It is the guard period between time-slots for power ramping and no data are transmitted during this time.

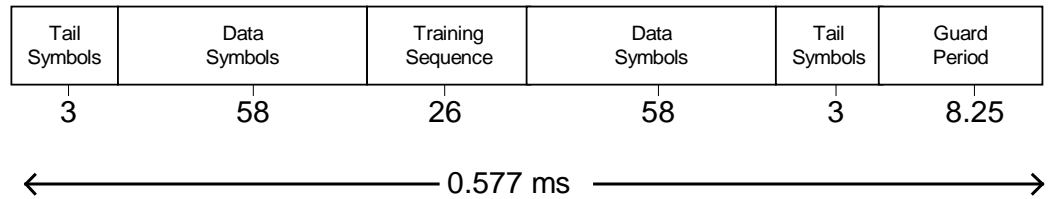


Figure 4. 1. Burst structure of EGPRS

The transmitted data symbols undergo severe Inter Symbol Interference (ISI) whose length is up to 7 symbol intervals for the worst case scenario in GSM

channel conditions. Therefore, a reliable and effective channel estimation and channel equalizer must reside for successful demodulation information data. The channel equalizer is designed to jointly eliminate the ISI and/or estimate the transmitted symbol sequence. As mentioned previously, the optimum equalization is performed by Maximum Likelihood Sequence Estimation (MLSE) for minimizing the probability of sequence error. The MLSE equalizer was widely postulated as a suitable technique for GSM radio with binary GMSK modulation scheme, where the MLSE equalizer's computational complexity is of the order 2^L per received data symbols with L being the channel memory. However for 8 PSK, the MLSE equalizer's computational complexity is of the order of 8^L per received data symbol, which is too high for practical implementations. Therefore, reduced state trellis-based equalizer's or symbol-by-symbol equalizers can be considered to overcome complexity drawback. Among the set of trellis-based reduced states equalizer's, the DDFSE appears as the one of the most suitable candidate because of its high regular structure, and good performance it provides, in regard with its moderate complexity [11][31]. Also performance is significantly better than that of simpler schemes such as DFE and LE [11][32] due to characteristic of mobile channel and dense signal constellation. Hence DDFSE is chosen as equalization scheme for 8 PSK modulation. Since high computational complexity is also the problem for the turbo detection, DDFSE is used in equalization part of the iterative scheme to reduce complexity by reducing the state of trellis.

Before the equalization and turbo decoding is investigated, a more detailed view of modulation and coding schemes for EGPRS with the characteristic of the GSM channel conditions is given firstly.

4.1 Modulation Coding Schemes of EGPRS

In EGPRS, nine modulation and coding scheme are specified [23]. Four schemes (MCS-1,...,MCS-4) employ GMSK modulation, while 8-PSK is used in other five (MCS-5,...,MCS-9). Each scheme employs the same convolutional code with code rate 1/3. However MCSs have different code rates as in Table 4.1 which are obtained by puncturing with different patterns.

Table 4.1. Modulation and coding schemes (MCS) for EGPRS

Scheme	Modulation	Code rate
MCS-9	8PSK	1.0
MCS-8	8PSK	0.92
MCS-7	8PSK	0.76
MCS-6	8PSK	0.49
MCS-5	8PSK	0.37
MCS-4	GMSK	1.0
MCS-3	GMSK	0.80
MCS-2	GMSK	0.66
MCS-1	GMSK	0.53

These different code rates and modulation types allow flexible adaptation of data throughput on a channel conditions by link adaptation and incremental redundancy techniques. The raw user data is combined with some header and indicator fields yielding fixed size data blocks. The length of user data in these data blocks is different for each MCS, i.e. 209 user bits are inserted in data block for MCS-1 while 1228 bits is processed for MCS-9. Each data block is first block encoded to produce parity bits of the length 12 for data and 8 for header parts for the purpose of error detection. Since block decoding scheme is not employed in equalization and turbo detection, the

behavior of the block codes is not investigated in this thesis. After block encoding, information and parity bits are encoded with a 1/3 rate convolutional code whose generator matrix $G(D)$ is given by

$$G(D) = \begin{pmatrix} 1 + D^2 + D^3 + D^5 + D^6, & 1 + D + D^2 + D^3 + D^6, & 1 + D + D^4 + D^6 \end{pmatrix} \quad (4-1)$$

Encoded sequence is then punctured to obtain desired code rates (Table 4.1). Each MCS has different puncturing sequences, P_1, \dots, P_n , resulting in the same code rate but a difference in transmitted bits. For example, first puncturing scheme, P_1 , for MCS-9 allows c_{3k} being transmitted while P_2 results in transmission of c_{3k+1} , and P_3 corresponds to c_{3k+2} transmission, where c represents convolutional encoded information sequence. Finally, the puncturing sequence is interleaved according to the corresponding rule in [23] and mapped on the burst structure of EGPRS. For example, the operations to construct MCS-5 are summarized in Figure 4. 2.

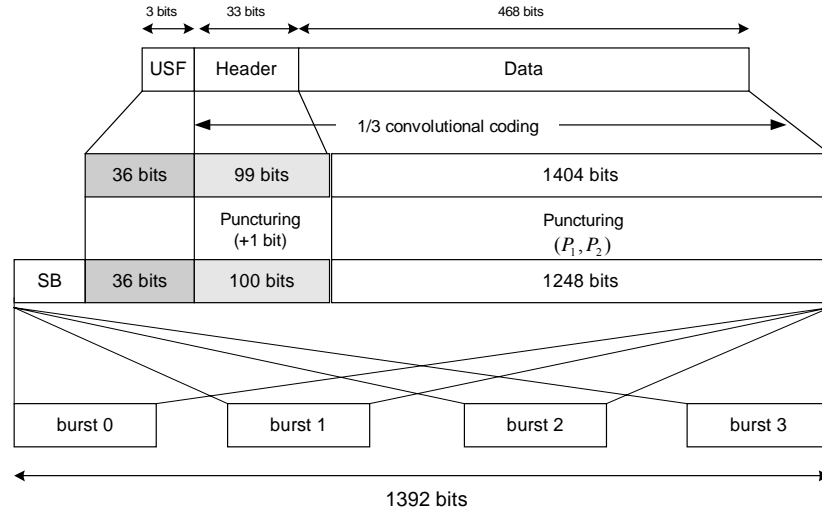


Figure 4. 2. Operations to construct MCS-5

4.1.1 Modulation Format of EGPRS

The core issue in EDGE, hence in EGPRS, is the introduction of a high order modulation technique. EDGE improves spectral efficiency by applying 8-ary phase-shift keying (8 PSK). Since it also uses binary Gaussian minimum-shift keying (GMSK) as GSM, both modulation types are explained in the following lines briefly.

4.1.1.1 Gaussian minimum-shift keying

GMSK is a special type of continuous phase modulation (CPM) with modulation index $h = 1/2$ and with a Gaussian like frequency shaping pulse [19]. EDGE uses GMSK with a bandwidth data period product of $BT = 0.3$. This modulation type is non-linear. However, it can be represented as a linear modulation technique by the Laurent decomposition [20]. In this case, the GMSK signal in baseband can be expressed as;

$$x(t) = \sum_{i=-\infty}^{\infty} \exp\left(j \frac{\pi}{2} \sum_{k=-\infty}^i b_k\right) f(t-iT) \quad (4-2)$$

where b_k 's $\in \{\pm 1\}$ are the pre-coded code bits to the modulator and $f(t)$ denotes the real-valued pulse shaping function which has linearized Gaussian pulse shape and spans a time interval of approximately 4 symbol durations. The explicit expression of $f(t)$ can be found in [19].

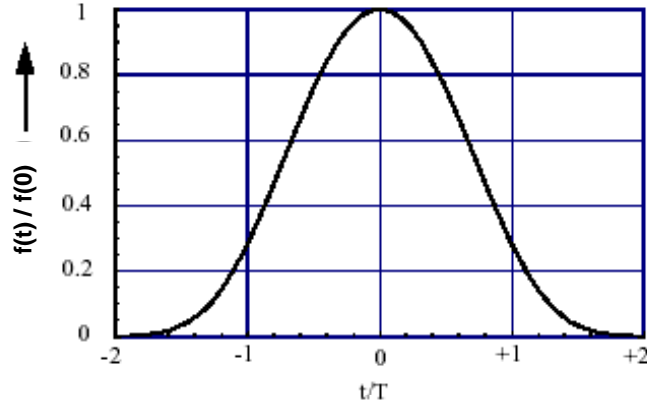


Figure 4. 3. Linearized gaussian shaping function

The expression for $x(t)$ in eq. (4.2) can be simplified by substituting $b_k = c_k c_{k-1}$. By assuming that the data sequence b_k is defined for $k \geq n_0$, n_0 being an arbitrary integer, equation (4.2) can be rewritten as;

$$\begin{aligned}
 x(t) &= \sum_{i=n_0}^{\infty} \exp \left(j \frac{\pi}{2} \sum_{k=n_0}^i c_k c_{k-1} \right) f(t - iT) \\
 \Rightarrow x(t) &= \sum_{i=n_0}^{\infty} \prod_{k=n_0}^i \exp \left(j \frac{\pi}{2} c_k c_{k-1} \right) f(t - iT)
 \end{aligned} \tag{4-3}$$

Substituting $\exp \left(j \frac{\pi}{2} c_k c_{k-1} \right) = jc_k c_{k-1}$, then, the equation (4.3) can be rewritten as;

$$x(t) = \sum_{i=n_0}^{\infty} \prod_{k=n_0}^i jc_k c_{k-1} f(t - iT) \tag{4-4}$$

Noticing that,

$$\prod_{k=n_0}^i c_k c_{k-1} = c_{n_0-1} c_{n_0} c_{n_0} c_{n_0+1} c_{n_0+1} c_{n_0+2} \dots c_{i-2} c_{i-1} c_i = c_i c_{n_0-1} \prod_{k=n_0}^{i-1} c_k^2 = c_i c_{n_0-1}$$

and dropping the terms that are independent of i gives;

$$x(t) = \sum_{i=n_0}^{\infty} c_i j^i f(t-iT) \quad (4-5)$$

The starting time index n_0 can be set to $-\infty$ which yields a general result as;

$$x(t) = \sum_{i=-\infty}^{\infty} c_i j^i f(t-iT) \quad (4-6)$$

Equation (4.6) shows that the modulated signal can be simply approximated by convolving the input data with pulse shaping function $f(t)$ and applying a phase rotation of $\pi/2$ radians.

4.1.1.2 8-ary Phase Shift Keying

The modulation currently being considered for EDGE is $3\pi/8$ offset 8-PSK with linearized GMSK pulse shape with symbol period of $3.69 \mu s$ [22]. In figure 4.4, modulator in base band description is depicted.

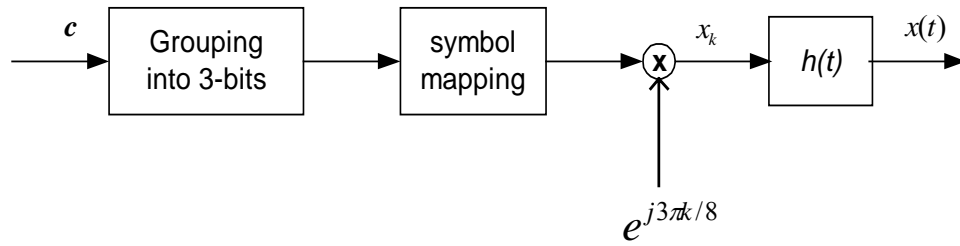


Figure 4. 4. 8 PSK modulator

The incoming coded bit sequence c is split into block of 3 bits and is mapped onto 8 PSK symbols, x , using gray encoding in figure 4.5. Then, each phase modulated symbol is shifted by $3\pi/8$ times symbol index. The resulting symbols represented by dirac pulses excite the linearized gaussian pulse shaping filter which has the shape in figure 4.3 [21].

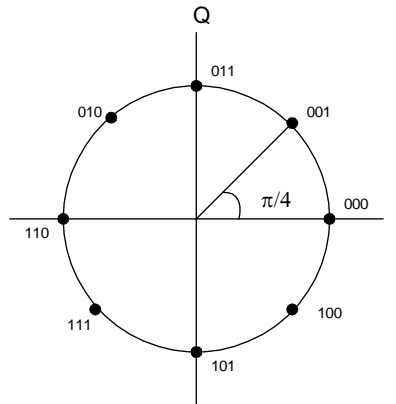


Figure 4. 5. 8 PSK constellation

Hence complex envelope of the modulated signal:

$$x(t) = \sum_k x_k h(t - kT) \quad (4-7)$$

where $x_k = e^{j\left(\frac{\pi}{4}d_k + \frac{3\pi}{8}k\right)}$ with $d_k \in \{0, \dots, 7\}$ and $h(t - kT)$ is shaping filter.

4.2 Mobile Radio Channel

In radio propagation channels, the transmitted radio signal may be obstructed by buildings, foliage, or other objects, which result reflections, scattering and diffraction. As a consequence, the propagating signal arrives at the receiver with multiple components of transmitted waveform, which is attenuated and delayed in time. This is called as multipath phenomenon and the delayed replicas of the transmitted signal can cause inter symbol interference in the receiver according to delay spread of the channel and the symbol period of the transmitted signal.

The mobile radio channel is also time-varying due to mobility of either the transmitter or the receiver or even of the surrounding objects. Whenever there is a relative motion between transmitter and receiver, the received carrier frequency is shifted relative to the transmitted carrier frequency. This shift of frequency is called the Doppler frequency shift f_d . In reality the received signal arrives from multiple paths and the velocity of movement in the direction of each path is usually different from that of another path. Therefore, the received signal of a transmitted sinusoid will have a spectrum composed of frequencies in the range $f_c - f_d$ to $f_c + f_d$. This spectrum is

referred to as the Doppler spectrum. Doppler spectrum is a measurement of the spectral broadening caused by the rate of change in the mobile radio channel.

A mobile radio channel can be represented with a tapped delay line model as in figure 4.6 for practical simulation.

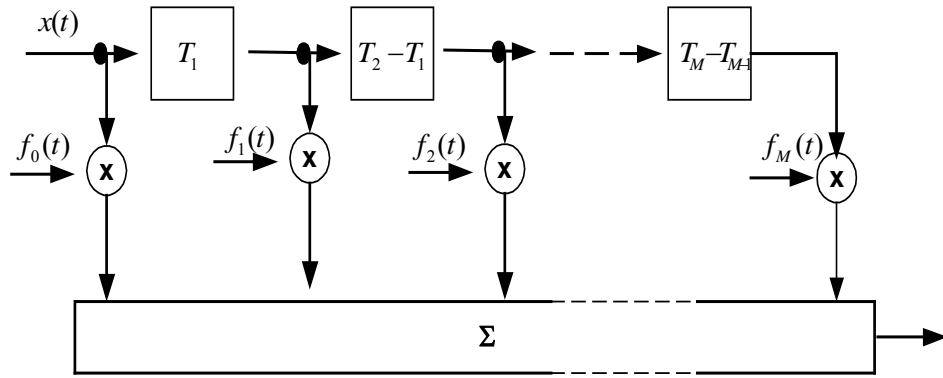


Figure 4. 6. Tapped delay line model of mobile channel

In this figure, the time delays and the average powers of the taps are described by propagation models and the channel tap gains vary according to doppler spectrum [19]. For GSM channel conditions, three propagation models are defined. These models are typical case for Rural Area (RA), Typical case for Urban area (TU) and typical case for Hilly Terrain (HT) whose multipath profiles in 6-taps settings are depicted in figures 4.7 to 4.9. As seen the figures, the delay spread varies from $0.7 \mu\text{s}$ to $17.2 \mu\text{s}$ depending on the channel model.

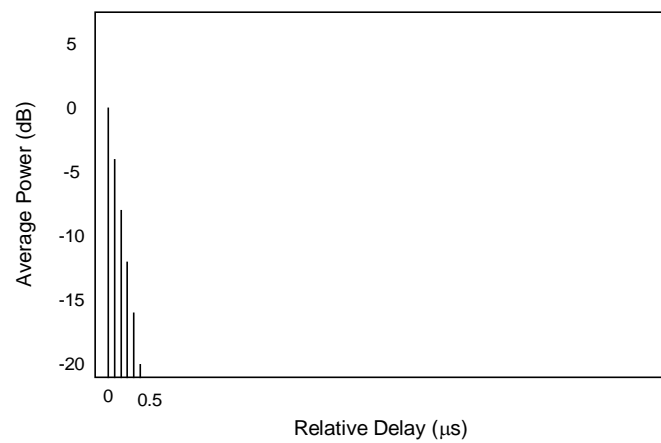


Figure 4.7. Rural Area Propagation Model

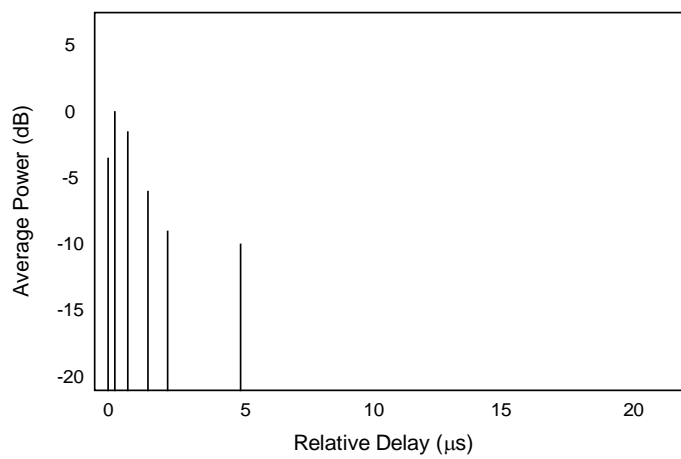


Figure 4.8. Typical Urban Propagation Model

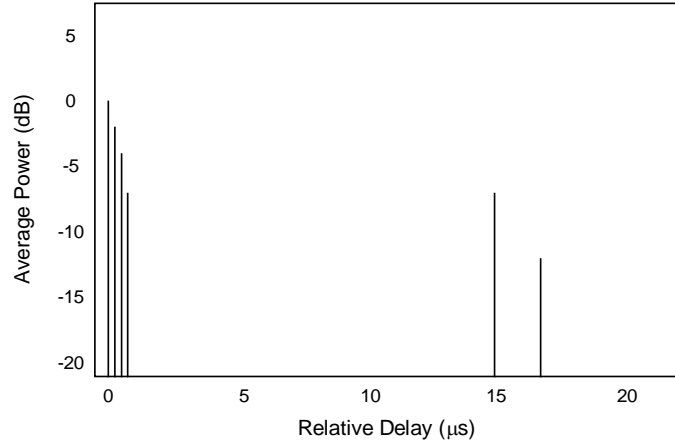


Figure 4.9. Hilly Terrain Propagation Model

Two types of Doppler spectra are defined in GSM standards to define variation of each tap. These are classical Doppler spectrum, abbreviated as CLASS and the Rice spectrum abbreviated by RICE. The CLASS type are used for all cases except for the shortest path of the model for propagation in rural areas and the spectra is given by:

$$S(f) = \frac{1}{\sqrt{1 - \left(\frac{f}{f_d}\right)^2}} \quad (4-8)$$

$$f \in (-f_d, f_d)$$

where f_d is the Doppler shift which is given by $(v/c)f_c$, where v is the mobile speed, c is the velocity of light and f_c is the carrier frequency.

The RICE type is only used for the shortest path of the rural area propagation and is the sum of a classical Doppler spectrum and one direct path such that

the total multi-path contribution is equal to that of the direct path. The spectrum expression is given by:

$$S(f) = \frac{0.41}{2\pi f_d \sqrt{1 - \left(\frac{f}{f_d}\right)^2}} + 0.91\delta(f - 0.7f_d), f \in (-f_d, f_d) \quad (4-9)$$

4.3 Receiver Structure

As can be seen from Fig 4.10, when modulated data is transmitted to the receiver through a mobile radio channel, ISI and additive noise destroy the transmitted signal. For GSM channel conditions, delay spread can rise up to 17.2 μ s in hilly terrain (HT) areas for 6-tap settings. In this case, with the symbol interval of 3.69 μ s, the transmitted signal undergoes the ISI with length up to 7 symbol which is due to both delay spread of the mobile channel and the partial response of the shaping filter.

Therefore, to estimate the transmitted, effective equalizer must be employed. However, due to the 8-ary symbol alphabet of EGPRS, the full state trellis structure is too complex for equalization issue and the DDFSE can be implemented as a suboptimal and less complex trellis based scheme as mentioned previously.

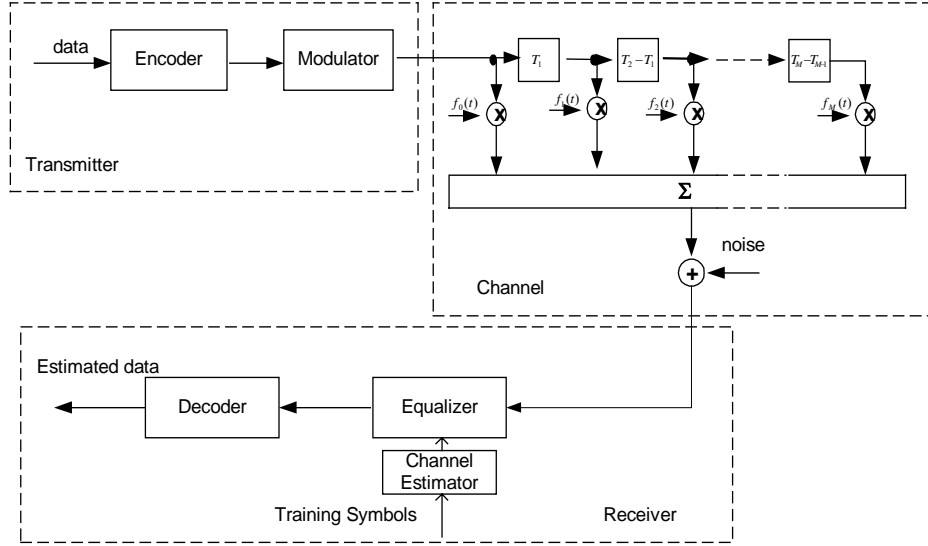


Figure 4. 10. Block diagram of transmission model under consideration

4.3.1 Channel Estimation

The DDFSE requires knowledge on the channel impulse response as other trellis based equalizers. The known training sequence of symbols in the middle of the each burst as presented in figure (4.1) and the corresponding received samples are utilized for estimating the Channel Impulse Response (CIR) for each burst separately. For this purpose the Least-Squares (LS) approach can be considered for channel estimation [16] and can be summarized as in following lines;

The received signal \mathbf{r} can be expressed as follows

$$\mathbf{r} = \mathbf{M}\mathbf{h} + \mathbf{z} \quad (4-10)$$

Where the complex channel impulse response \mathbf{h} of the wanted signal is expressed as

$$\mathbf{h} = [h_0 \ h_1 \ \text{K} \ \text{K} \ h_L]^T \quad (4-11)$$

and \mathbf{z} denotes the noise samples.

The unique training sequence for each transmission is divided into a reference length of P and guard period of L bits where $P+L-1=25$, and denoted by

$$\mathbf{m} = [m_0 \ m_1 \ \text{K} \ \text{K} \ m_{P+L-1}]^T \quad (4-12)$$

where $m_i \in \{-1, +1\}$. Finally the circulate training sequence matrix \mathbf{M} is formed as

$$\mathbf{M} = \begin{bmatrix} m_L & \Lambda & m_1 & m_0 \\ m_{L+1} & & m_2 & m_1 \\ \text{M} & & \text{M} & \text{M} \\ m_{L+P-1} & \Lambda & m_P & m_{P-1} \end{bmatrix} \quad (4-13)$$

The LS channel estimates are found by minimizing the following quantity

$$\mathbf{h} = \arg \min_h \|\mathbf{r} - \mathbf{M}\mathbf{h}\|^2 \quad (4-14)$$

The solution assuming noise z is white gaussian is given by following equation

$$\hat{\mathbf{h}}_{LS} = (\mathbf{M}^H \mathbf{M})^{-1} \mathbf{M}^H \mathbf{r} \quad (4-15)$$

where $()^H$ and $()^{-1}$ denote the hermitian and inverse matrices, respectively. For the EGPRS systems, the given solution is further simplified to

$$\hat{\mathbf{h}} = \frac{1}{P} \mathbf{M}^H \mathbf{r} \quad (4-16)$$

because the correlation matrix $\mathbf{M}^H \mathbf{M}$ becomes diagonal, provided that the periodic auto-correlation function (ACF) of the training sequence is ideal with the small delays from 1 to L . This holds for GSM training sequences, whenever reference length 16 is chosen and for $0 \leq L \leq 5$. The estimates given by the last equation are simply scaled correlations between the received signal and training sequence.

4.3.2 Delayed Decision Feedback Sequence Estimation for EGPRS

As mentioned in section 2.3, the DDFSE reduces the receiver complexity by truncating the effective channel memory to μ terms, where μ is an integer that can be varied from 0 to L . Since only the μ most recent symbols are processed by sequence estimation, it is important to have most of the signal energy contained in these terms. Hence, in order to obtain a high performance, the channel impulse response, \mathbf{h} , seen by equalizer should have

a have minimum phase characteristics. To accomplish this task, a whitening match filter can be used before the DDFSE [35][33][24].

An ideal prefilter $A(z)$ should generate the minimum phase equivalent of $H(z)$

$$H_{\min}(z) = \sum_{k=0}^L h_{\min}[k]z^{-k} \quad (4-17)$$

with

$$H_{\min}(z) \cdot H_{\min}^*(1/z^*) = H(z) \cdot H_{\min}^*(1/z) \quad (4-18)$$

where $H_{\min}(z)$ has roots only inside and on the unit circle, keeping energy in the tail of $h_{\min}[\cdot]$ to minimum. The transfer function of this filter can also be represented as

$$A(z) = \frac{H_{\min}(z)}{H(z)} = A_1(z) \cdot A_2(z) \quad (4-19)$$

$$A_1(z) = H^*(1/z^*) \quad (4-20)$$

$$A_2(z) = \frac{1}{H_{\min}^*(1/z^*)} \quad (4-21)$$

Hence, $A(z)$ may be viewed as a cascade of two filters $A_1(z)$ and $A_2(z)$ [27]. For a given FIR channel, the impulse response of the filter $A_1(z)$, is given by the complex-conjugated and time-reversed channel impulse-response, i.e., $A_1(z)$ is a matched filter, matched to the discrete-time channel impulse response. Thus, the remaining problem consists transfer function

$A_2(z)$, which may be viewed as a noise whitening filter. The wiener solution for whitening filter is given in [25] as

$$\begin{bmatrix} \psi_{-N,-N} & K & \psi_{-N,0} \\ M & O & M \\ \psi_{0,-N} & K & \psi_{0,0} \end{bmatrix} \begin{bmatrix} a_{-N} \\ M \\ a_0 \end{bmatrix} = \begin{bmatrix} \rho_{-N} \\ M \\ \rho_0 \end{bmatrix} \quad (4-22)$$

with elements of Hermitian matrix ψ .

$$\psi_{i,j} = \sum_{l=L}^{-j} \rho_l \rho_{l+j-i}^* \quad (i, j = -N, K, 0) \quad (4-23)$$

where ρ is auto-correlation sequence of channel impulse response and N is whitening filter length and \mathbf{a} constitutes coefficients of the whitening filter. If channel noise is also taken into account, the matrix entries are modified to the

$$\psi_{i,j} = \sum_{l=L}^{-j} \rho_l \rho_{l+j-i}^* + \frac{1}{\gamma} \rho_{i-j} \quad (i, j = -N, K, 0) \quad (4-24)$$

to obtain the MMSE whitening filter where γ is the symbol SNR.

In the EGPRS transmission format, separate equalization processes, starting from the edges of the training sequence and proceeding in positive and negative time direction respectively, are applied as in figure (4.11) where training sequence produces the initial states for the trellis based equalizer and the channel knowledge is better.

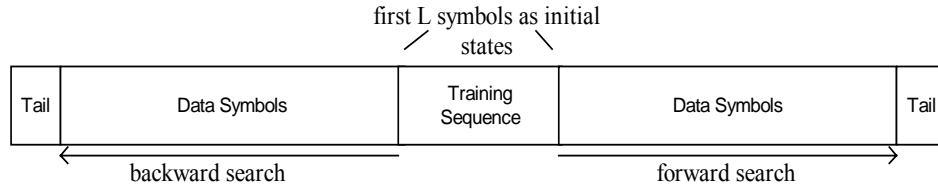


Figure 4.11. Estimation of the data symbols in the burst

The prefilter described above that transforms CIR into minimum-phase is used for equalization in positive time direction. For equalization in negative time direction, a maximum phase overall impulse response is required. This can be generated by another prefilter whose transfer function expressed as follows [27]

$$\tilde{A}(z) = H^*(1/z^*) \cdot A_2^*(1/z^*) \quad (4-25)$$

After prefiltering, the DDFSE algorithm whose details is given in section 2.3 is used to equalize the received symbols.

Three channel profiles described in section 4.2 with mobile speed of 3km/h are used to observe effect of the channel types on the performance on the DDFSE equalizer. For RA and TU profiles, an equalizer which copes with 4 ISI terms is adequate to compensate the time dispersion introduced by the transmitter and the radio channel. However, the received signal transmitted through HT area undergoes more severe ISI corresponds to 7 symbol duration.

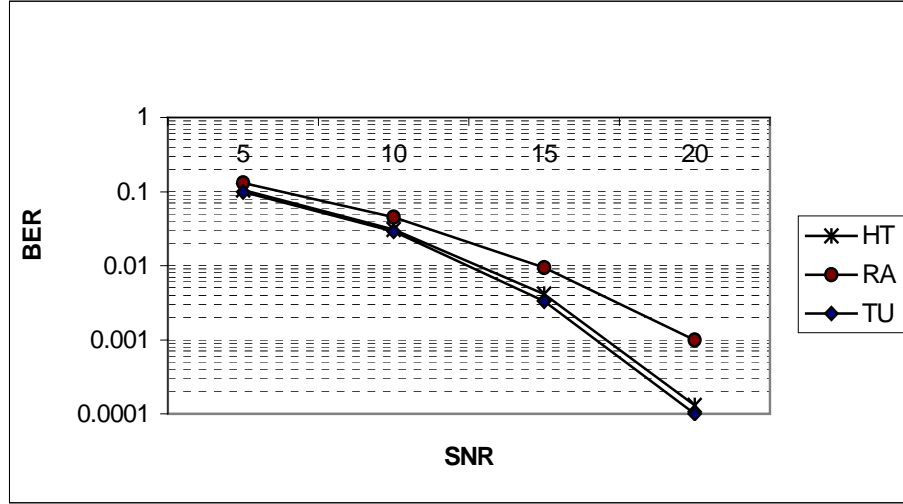


Figure 4. 12. BER performance of DDFSE equalizer with $\mu=2$

The figure (4.12) shows the bit error rate (BER) vs. SNR curves for the channel profiles typical urban (TU), hilly terrain (HT) and rural area (RA). The worst performance is observed for the RA profile since path diversity is minimum for this profile, the all signal power is concentrated in a very short time period, therefore the receiver, in general, picks the signal from one path only. When this path fades, the performance of the receiver severely degrades. The time spread of the channel provides a sort of time diversity since the probability that all the signal paths fade simultaneously is fairly low. Therefore, the best performance is expected to attain for HT channels whose time dispersion extends up to 5 symbols duration. However, since the number of taps of channel impulse response and their energy employed in the feedback path in the DDFSE algorithm is higher for the HT profile than that

of the TU, similar BER performances are obtained for the HT and the TU channels.

The complexity of the receiver, which tries to combat ISI produced by the HT, is higher comparing to the one designed for the TU profile due to long channel impulse response which results in higher complexity in the DDFSE algorithm, channel impulse response estimation and prefiltering process. Therefore, the TU power profile is chosen to determine the effect of trade off parameter μ on the performance of the DDFSE receiver, since the RA profile has too low time dispersion to examine the performance of a DDFSE receiver.

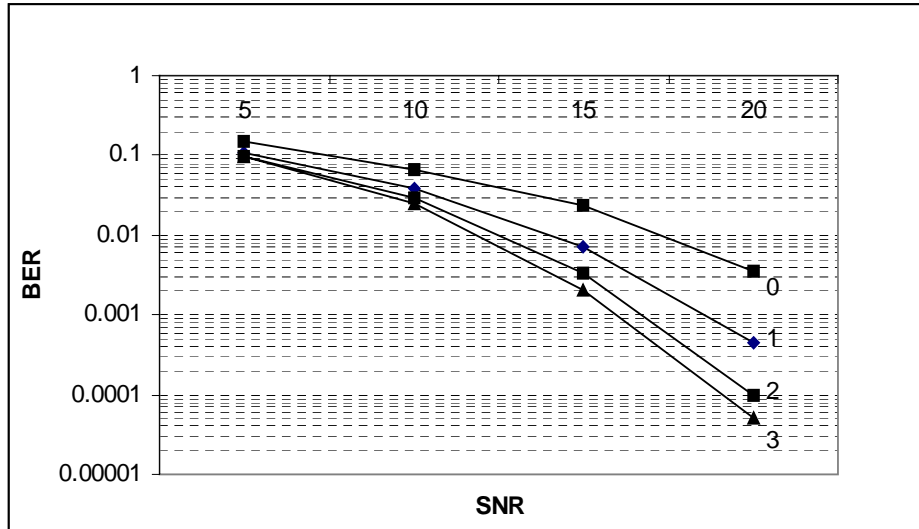


Figure 4. 13. BER performance of DDFSE equalizer with $\mu= 0,1,2,3$

Figure (4.13) shows BER performance comparison of DDFSE equalizers with different values of μ ranging from 0 to 3. Channel is assumed stable within a burst in the simulation. As the number of states processed in Viterbi structure increases, BER of the DDFSE scheme improves, since error propagation plays a crucial role especially for small μ . For instance, at $\text{BER}=10^{-2}$ DDFSE scheme with $\mu=2$ yields approximately 5dB gain compared to DDFSE scheme with $\mu=0$. According to figure (4.13), for $\mu=3$ only slight improvement can be obtained over $\mu=2$ with high computational complexity. Hence $\mu=2$ seems to provide a good tradeoff between performance and complexity for the DDFSE.

4.3.3 Turbo Detection for EGPRS

The turbo detection scheme defined in chapter 3 is utilized for EGPRS with DDFSE scheme to reduce the number of the trellis states in the SISO equalizer. Max-log-MAP algorithm, which has low computationally complexity compared to the optimum MAP algorithms with only slight performance degradation [14] is employed both in detection and decoder parts.

Decoding is performed over full state trellis which is constructed by state sequence $s_k = (u_{k-1}, K, u_{k-K+1})$ while \mathbf{u} is information bit sequence and $K=7$ is constraint length of the convolutional coding, by applying algorithm expressed in section 3.2.2.

Equalization is employed by applying Max-Log-MAP over reduced state structure of DDFSE algorithm. For this purpose, the backward transition

probabilities in equation (3.16) are first computed using the branch transition probability expression in equation (4.26) and partial states are determined for each state in DDFSE structure as described in section (2.3).

$$\overline{\mu}_k(s_k^{\mu(i)} \rightarrow s_{k+1}^{\mu(j)}) = -\frac{1}{2\sigma^2} \left| r_k - h_0 x_k(s_k^{\mu(i)} \rightarrow s_{k+1}^{\mu(j)}) - \sum_{l=1}^{\mu} h_l x_{k-l}(s_k^{\mu(i)}) + \hat{w}_k \right|^2 + L_e^D(x_k)$$

(4- 26)

Then, with the partial states estimated in forward tracing, the backward transition probabilities are calculated using equation (4.26) and L-values are obtained as in section 3.2.3. Since nonbinary modulation scheme is considered, the approach in section 3.2.3, is applied to compute the symbol L-values in equation (4.26).

The TU channel profile is used to simulate turbo detection scheme as suggested in previous section with μ as 2, since it provides a good tradeoff between performance and complexity (see figure 4.13). Before examining turbo detection scheme, the performance of the conventional receiver structure, which provides the estimates of information bits without any iteration is observed and the results is given in the following figure.

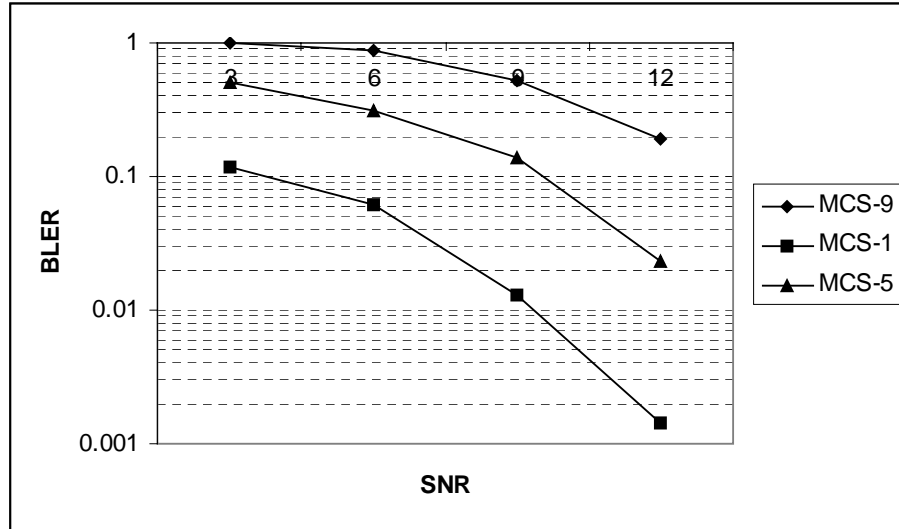


Figure 4. 14. BLER for conventional EGPRS receiver with different MCSs

Figure (4.14) shows BLER, the block error rate, referring to all erroneously decoded data blocks, for MCS-1 which utilize GMSK modulation with coding rate 0.53, MCS-5 with 8-PSK with coding rate 0.37 and MCS-9 whose coding rate is 1. As can be noticed, the performance of EGPRS receiver depends on modulation and coding schemes. Increase in coding rate significantly degrades the performance of the decoder blocks (see MCS-5 and MCS-9 curves) while increase in modulation level results in decrease in reliability of the equalizer output feed to decoder (see MCS-1 and MCS-5 curves).

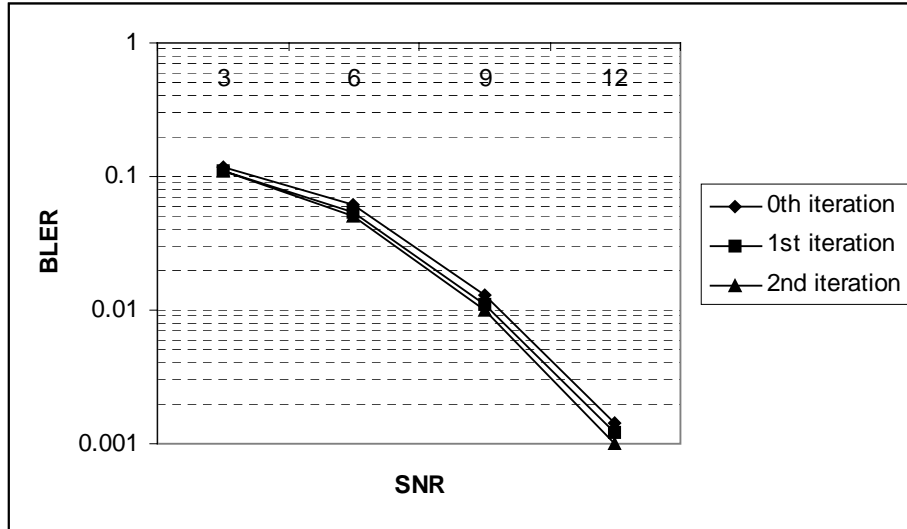


Figure 4.15. Turbo detection performance for MCS-1

The turbo detection scheme is first examined for MCS-1, which employ GMSK modulation and as seen from figure (4.15), only small iteration gains are achieved. Only around 0.3 dB gain at BLER 10^{-2} after first iteration and totally around 0.4 dB gain after second iteration are observed. Since GMSK is a binary modulation type, the impact of the ISI is reduced significantly in equalizer and soft information output is highly reliable even in the 0th iteration.

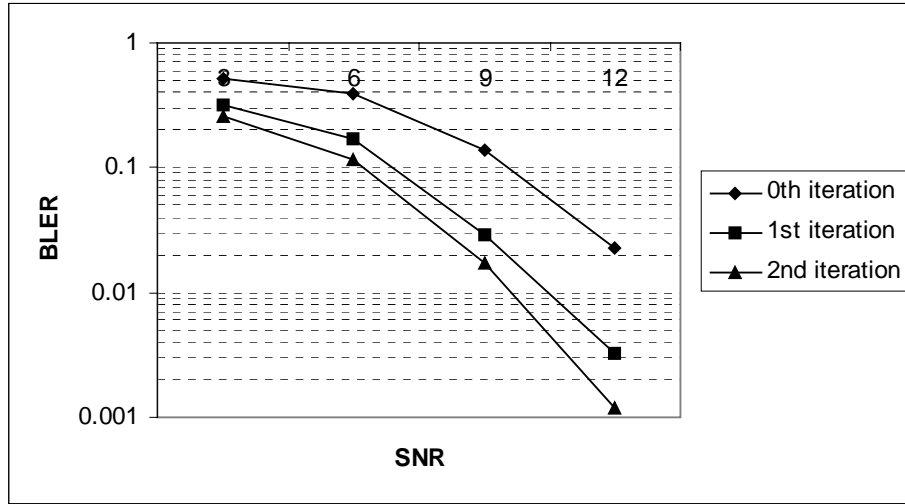


Figure 4. 16. Turbo detection performance for MCS5

Better results for the BLER are obtained for MCS-5 as shown in figure 4.16. At the BLER of 0.1, a gain of 3dB can be achieved with two iterations. The largest gain of 3.6 dB is obtained on the first iteration whereas second iteration only improves the BLER by 0.6 dB.

The iteration gain is obviously higher for MCS-5, when compared to MCS-1. This is due to higher-order modulation employed in MCS-5, 8PSK, with respect to MCS-1 whose modulation mode is binary. The Euclidean distance between two neighborhood points in 8-PSK constellation is smaller and hence it is more gravely affected by ISI and noise. Consequently the BER performance of SISO equalizer at 0th iteration incurred higher degradation, when compared to more robust lower level modulation mode GMSK. However, the impact of ISI was reduced significantly for the subsequent iteration, which results in high iteration gain for MCS-5. This can be seen in

figure 4.17, which shows BER performance of the SISO equalizer at 3 turbo iterations.

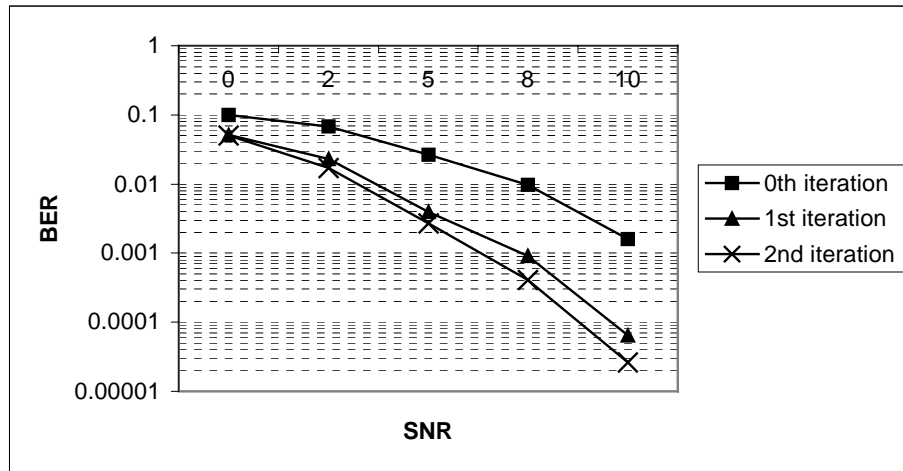


Figure 4. 17 Raw BER after equalizer for MCS5

CHAPTER 5

CONCLUSION

In this thesis, equalization and turbo detection for EGPRS has been considered. Because of the high level modulation applied in EGPRS, compared to GSM case, computational complexity prevents receiver from employing an optimum equalization scheme. For the practical implementation, reduction in complexity of the equalizer is required without significant degradation in the bit error rate. Therefore, the DDFSE equalizer is investigated in this thesis for 8-PSK modulation as reduced state trellis based equalizer scheme. It is shown by simulation results that the DDFSE provides a fine tradeoff between performance and complexity and it is attractive solution even with only a few numbers of states.

The turbo detection performance is examined for EGPRS by adopting DDFSE scheme in equalizer part to reduce extensive computational load of the SISO equalizer. Simulation results show that Turbo detection provides an iteration gain compared to the conventional equalization and decoding structure. The iteration gain depends on modulation type. It sufficiently improves the performance of MCS, which employ 8-PSK modulation, while it is very low for MCS of GMSK modulation. Additionally, The efficiency of

turbo detection heavily depends on coding scheme. In the case of the coding rate is very high i.e., MCS9 which have a coding rate of one, turbo detection yields no gain at all.

This thesis attempts to examine the performance of a reduced complexity equalizer, the DDFSE, and that of the turbo detection for EGPRS. The time invariant channel conditions are assumed and channel impulse response is estimated in burst by burst basis, however at high vehicle speeds imperfect tracking of the channel causes performance degradation in the detection scheme. It would be useful to employ an adaptive channel tracking algorithm to compensate this type of degradation for fast fading conditions.

Additionally, incremental redundancy scheme for EGPRS can be studied to increase an iteration gain for modulation coding scheme with high coding rate and to examine performance of the EGPRS receiver as further a research area.

REFERENCES

- [1] Siemens white paper, “3G Wireless Standards for Cellular Mobile Services”, 2002
- [2] “Evaluation of TDMA-Based 2G Systems to 3G Systems, Wireless Network Evolution: 2G to 3G”, <http://www.phptr.com>, June 2001
- [3] C. Bettstetter, H.J. Vögel, and J. Eberspacher, “GSM Phase 2+ General Packet Radio Service GPRS: Architecture, Protocols, and Air Interface”, IEEE Commun. Surveys, vol. 2, no. 3, Third Quarter 1999
- [4] D. Molkdar, and V. Featherstone “System Level Performance Evaluation of EGPRS in GSM Macro Cellular Environments”, IEEE VTSL, vol. 6, pp. 2653 –2660, Sept. 2000
- [5] A. Furuskär, S. Mazur, F. Müller, and H. Olofsson, “EDGE: Enhanced Data Rates for GSM and TDMA/136 Evolution,” IEEE Pers. Commun., vol. 6, pp. 56–66, June 1999
- [6] C. Lindheimer, S. Mazur, J Molnő, and M. Waleij, “Third-Generation TDMA”, Ericsson Review, no. 2, 2000

- [7] J. G. Proakis, "Digital Communications", 3rd ed. New York: McGraw-Hill, 1995
- [8] G. L. Stuber, "Principles of Mobile Communication" Kluiver Academic Publishers, 1996
- [9] L. Hanzo, C. H. Wong, and M. S. Yee, "Adaptive Wireless Transceivers" IEEE press John Wiley and Sons LTD, 2002
- [10] A. Duel, and C. Heegard, "Delayed Decision-Feedback Sequence Estimation," IEEE Trans. on Commun., vol.37, no.5, May 1989
- [11] W. H. Gerstacker, and R. Schober, "Equalization Concepts for EDGE", IEEE Trans. Wireless Commun., vol. 1, no. 1, Jan. 2002
- [12] C. Douillard, M.Jézéquel, C.Berrou, A.Picart, P.Didier, and A.Glavieux, "Iterative Correction of InterSymbol Interference: Turbo-Equalization", European Trans. Telecommun., vol. 6, pp. 507-511, Sept. 1995
- [13] L. R. Bahl, J. Cocke, F. Jelinek, and J. Raviv, "Optimal Decoding of Linear Codes for Minimizing Symbol Error Rate," IEEE Trans. Info. Theory, vol. IT-20, pp. 284–287, Mar. 1974
- [14] G. Bauch, and V. Franz, "A Comparison of Soft-In-Soft-Out Algorithms for Turbo-Detection", ICT, vol. 2, pp. 259-263, Portos Carras, Greece, June 1998

- [15] S. H. Müller, and W. H. Gerstacker, and J. B. Huber, “Reduced-State Soft-Output Trellis-Equalization Incorporating Soft Feedback”, GLOBECOM, vol. 1, pp. 18-22, Nov. 1996
- [16] V. Franz, G. Brauch, “Turbo-Detection for Enhanced Data GSM Evolution“, IEEE VTC, vol. 4, pp. 2954-2958, Amsterdam, Sept. 1999
- [17] P. Strauch, C. Luschi, and A. M. Kuzminskiy, “Iterative Channel Estimation for EGPRS”, IEEE VTS, vol. 5 , pp. 2271 -2277, Sept. 2000
- [18] S. H. Redl, M. K. Weber, M. W. Oliphant, “An Introduction to GSM”, Artech House, INC, 1995
- [19] S. K. Eken, “A Study on GMSK and Channel Simulation”, MS Thesis in Electrical and Electronics Engineering METU, 1994
- [20] P. A. Laurent, “Exact and Approximate Construction of Digital Phase Modulation by Superposition of Amplitude Modulated Pulses (AMP)”, IEEE Trans. on Commun., 34, 150, Feb. 1986
- [21] V. S. Stephan, “Implementation Effects on GSM’s EDGE Modulation”, Tropian Inc.
- [22] ETSI. GSM Recommendations 05.04 : Modulation, ver. 8.4.0, 1999
- [23] ETSI. GSM Recommendations 05.03 : Channel Coding, ver. 8.7.0, 1999

- [24] G. D. Forney, "Maximum-Likelihood Sequence Estimation of Digital Sequences in the Presence of Intersymbol Interference," IEEE Trans. Info. Theory, vol. IT-18, pp. 363–378, May 1972
- [25] B. Baykal, "Blind Matched Filter Receiver", IEEE Trans. on Circuits and Systems-II, 2003
- [26] R. Visoz, A. O. Berthet, A. Saadani, and B. Penther, "Turbo Equalization and Incremental Redundancy for Advanced TDMA Systems", IEEE VTC, vol.3, pp. 1629 –1633, May 2001
- [27] W. H. Gerstacker, F. Obernosterer, R. Meyer, and J. B. Huber, "An Efficient Method for Prefilter Computation for Reduced-State Equalization", IEEE PIMRC vol.1, pp. 604 –609, Sept. 2000
- [28] M. Shafi, S. Ogoose, and T. Hattori, "Wireless Communications in the 21th Century", IEEE Press, 2002.
- [29] G. Bauch, H. Khorram, and J. Hangenauer, "Iterative Equalization and Decoding in Mobile Communication Systems", EPMCC, pp. 307-312, Bonn, Germany, Oct. 1997
- [30] W. Koch, and A. Baier, "Optimum and Sub-Optimum Detection of Coded Data Distributed by Time Varying Inter-Symbol Interference". IEEE GLOBECOM, vol.3, pp. 1679 –1684, Dec. 1990
- [31] A. Berthet, R. Visoz, P. Tortelier., "Sub-Optimal Turbo-Detection for Coded 8-PSK Signals over ISI Channels with Application to EDGE

Advanced Mobile System”, PIMRC 2000, vol.1, pp. 151 -157 , Sept. 2000

[32] J. C. Olivier, X. Chengshan, K. D. Mann, “An Efficient Equalizer for 8-PSK EDGE Cellular Radio System”, IEEE VTC-Spring, vol. 3, pp. 1668 –1672, May 2001

[33] M. Barberis, S. Heinen, P. Guerra, “Design of an Interference-Resistant Equalizer for EDGE Cellular Radio Systems”, VTC–Fall, vol. 3 , pp. 1622 -1626, Sept. 2002

[34] T. Xiang-guo, D. Zhi, “Turbo Equalization for EDGE System with DDF-SOVA”, Signals, Systems and Computers, vol. 1, pp. 295 –299, Nov. 2001

[35] N.H. Chow, T.G. Jeans, and R. Tafazolli, “Practical Reduced-Complexity Equalizer for EDGE”, Electronic Letters, vol.37, no.9, April 2001

[36] M. Pukkila, “Turbo Equalization for the Enhanced GPRS Systems”, PIMRC vol. 2, pp. 893-897, Sept. 2000